

Benthic methane fluxes and oxidation over the Western Indian Shelf: No evidence of pelagic methanotrophic denitrification

**Anil Pratihary^{1,2,*}, Damodar Shenoy¹, Jesly Araujo¹, Gayatri Shirodkar¹, Sunanda Sahu¹,
Manjima A.P.¹, Richita Naik^{1,3}, Supriya Karapurkar¹**

¹Chemical Oceanography Division, CSIR-National Institute of Oceanography,
Dona Paula, Goa, 403004, India

²Department of Biogeochemistry, Max-Planck-Institut für Marine Mikrobiologie,
Celsiusstraße 1,D-28359 Bremen, Germany

³Directorate of Fisheries, Govt. of Goa, Panaji, Goa, India

*Corresponding author: Email: apratihary@nio.res.in, Tel: +91-832-2450639

Abstract:

Despite its supersaturation in the waters and wide occurrence of gas-charged pockets in the sediments off Western India, methane occurs at unusually low concentrations in the shelf waters even during euxinic events, compared to other anoxic coastal systems of the world. To understand the reason and benthic biogeochemistry of CH₄, we measured benthic CH₄ flux rates through whole-core incubations, and carried out CH₄-spiked ¹⁵N-labeled incubations of the suboxic/anoxic shelf waters during 2011-2013. We observed very low rates of benthic CH₄ influx or efflux (-0.23 to 0.37 μmol m⁻² d⁻¹) during normoxia, and low to moderate rates of benthic CH₄ efflux (2.45 to 74.89 μmol m⁻² d⁻¹) during seasonal anoxia. However, high rates of the potential benthic CH₄ efflux (23.82 to 154.25 μmol m⁻² d⁻¹) implied massive benthic CH₄ oxidation. The diffusing CH₄ was oxidized within the sediments up to 99-100% during normoxia and up to 51-89% during anoxia. The benthic-released CH₄ was further oxidized in the water column aerobically at the rate of 0.84 μmol m⁻² d⁻¹ during normoxia, and anaerobically at the rate of 0.16 μmol m⁻² d⁻¹ during anoxia. However, we did not find any evidence for NO_x⁻ (NO₃⁻ and/or NO₂⁻)-dependent anaerobic CH₄ oxidation (N-DAMO) i.e. methanotrophic denitrification in the shelf waters during anoxia, which suggested the potential role of Fe³⁺ and Mn⁴⁺ and/or SO₄²⁻ as the alternative oxidants in the anaerobic CH₄ oxidation necessitating further research. The total annual benthic CH₄- flux rate and oxidation rate from the entire innershelf were estimated to be 9.45 Gg y⁻¹ and 30.71 Gg y⁻¹, respectively. Our study revealed that benthic- and pelagic anaerobic CH₄ oxidation combined together reduce the water column CH₄ concentration by 78-98%. Therefore the shelf sediments act as an effective CH₄ filter by substantially reducing the benthic CH₄ flux and ultimately the sea-air CH₄ emission.

Keywords: sediment, methane, flux, oxidation, shelf, India

1. Introduction

Methane is a potent greenhouse gas with 25 fold higher warming effect compared to CO₂ (Crutzen, 1991), and its atmospheric concentration has nearly tripled since pre-industrial times (1750 CE) reaching to the current (2018 CE) level of 1857 ppb (Saunio et al. 2020) although its rise had slowed significantly during late 1990's (Dlugokencky et al., 2001; Fiore et al., 2006). Globally, CH₄ is being emitted at the rate of 576 Tg y⁻¹ from various natural and anthropogenic sources, and the latter account for ~60% of the total CH₄ emission (Saunio et al., 2020). Global marine CH₄ emission has been estimated to be 5-17 (mean: 9) Tg y⁻¹ (Saunio et al., 2020) out of which coastal ocean contribute 50-80% despite covering only 15% of the total oceanic surface area (Steinle et al., 2017; Weber et al., 2019).

In marine environments, CH₄ is produced through microbial (archaeal) methanogenesis, a strictly anaerobic process which is inhibited by O₂ and SO₄²⁻ (Thauer et al., 2008; Garcia et al., 2000). Hence, methanogenesis widely occurs in anoxic marine sediments, and predominantly via CO₂ reduction (Eq. 1) rather than acetate fermentation (Eq. 2) pathway because of acetate depletion by SO₄²⁻ reducers (Reeburgh et al., 2007 and references therein).



Apart from microbial methanogenesis, leakage from cold seeps and destabilization of gas hydrates also contribute to the CH₄-supersaturation of sediment pore waters in some systems (Reeburgh et al., 2007; Mazumdar et al., 2009; Boetius and Wenzhöfer, 2013; Borges et al., 2016). Although, high CH₄ concentration is expected in the bottom waters in such shallow marine systems due to presumed high rate of benthic CH₄ efflux, the CH₄ build-up in the bottom waters are often reported to be low or moderate (Gülzow et al., 2013; Shirodkar et al., 2018; Mao et al., 2022; Lenstra et al., 2023) since ~90% of the microbially-produced CH₄ is oxidized within the sediments (Hinrichs and Boetius, 2002; Knittel and Boetius, 2009) by various bacteria and archaea anaerobically using oxidants e.g. SO₄²⁻ (Hinrichs et al., 1999; Boetius et al., 2000; Orphan et al., 2001), Mn⁴⁺ and Fe³⁺ (Beal et al., 2009), NO₃⁻ and NO₂⁻ (Raghoebarsing et al., 2006; Ettwig et al., 2008, 2010; Haroon et al., 2013), and aerobically using O₂ (Boetius and Wenzhöfer, 2013; Lenstra et al. 2023). The benthic-released CH₄ is also further oxidized in the water column aerobically (Mao et al., 2022) or anaerobically (Steinsdóttir et al., 2022a, 2022b) which significantly decreases the pelagic CH₄ inventory in the shallow marine systems. Thus, both benthic and pelagic methanotrophy act as methane filters and significantly reduce the CH₄ emission to the atmosphere. However, despite such high rate of benthic and pelagic CH₄

oxidation, oxygenated surface waters of numerous shallow coastal marine systems across the world have been reported to be supersaturated with CH₄ relative to its equilibrium concentration i.e. ~3 nM (Damm et al., 2015; DelSontro et al., 2018) thereby making them significant CH₄ emitters to the atmosphere (Brüchert et al., 2009; Naqvi et al., 2010; Gülzow et al., 2013; Borges et al., 2016; Shirodkar et al., 2018; Weber et al., 2019; Farias et al., 2021; Mao et al., 2022). This *methane paradox* (Reeburgh et al., 2007) is often explained by aerobic CH₄ production through (1) bacterial degradation of algal-derived methylated compounds e.g. methyl phosphonate (Karl et al., 2008; Arx et al., 2023), DMSP (Damm et al., 2010), phosphonate esters (Repeta et al., 2014), and methylamine (Wang et al., 2021), and (2) algal photosynthesis (Klitzsch et al., 2023).

The Western Indian Continental Shelf (WICS), the largest naturally-occurring seasonal anoxic coastal system of the world, is known as a major biogeochemical hotspot in the world ocean (Naqvi et al., 2006). The shelf experiences normoxia during November-May and suboxia/anoxia during June-October. The WICS waters have been often reported to be supersaturated with CH₄ i.e. up to 1041-2521% (Shirodkar et al., 2018; Jayakumar et al., 2001) with much higher degree of supersaturation i.e. up to 7456-10214% (Sudheesh et al., 2020; Arya et al., 2024) in the southern part of the WICS. Consequently, WICS has been designated as a significant emitter of CH₄ to the atmosphere as the sea-air CH₄ flux has been reported to be up to ~27 $\mu\text{mol m}^{-2} \text{d}^{-1}$ (Shirodkar et al., 2018) with much higher emission i.e. up to 170-756 $\mu\text{mol m}^{-2} \text{d}^{-1}$ in the southern part of the shelf (Sudheesh et al., 2022; Arya et al., 2023). The possible sources of CH₄ in the shelf waters have been hypothesized to be terrestrial run-off, sedimentary input and in-situ production from microniches (Jayakumar et al., 2001; Shirodkar et al., 2018; Sudheesh et al., 2022; Arya et al., 2023). However, the prime reason behind such high degree of supersaturation or the source of CH₄ in the water column has remained largely unknown, speculative and debatable so far. Besides, intriguingly, Shirodkar et al. (2018) reported abnormally low CH₄ build-up (<100 nM) in the sulfidic bottom water during seasonal anoxia which was much lower compared to other anoxic coastal systems of the world. Subsequently, Sudheesh et al. (2020) hypothesized CH₄ loss in the hypoxic/anoxic bottom waters through anaerobic CH₄ oxidation based on extremely low CH₄ accumulation in the southern region. However, no clear understanding exists as yet regarding the reason behind abnormally low CH₄ concentration reported during seasonal anoxia over the shelf.

We hereby hypothesize that although the shelf sediments have the potential to release significant quantity of CH₄ to the shelf waters, massive aerobic and anaerobic oxidation of the benthic-released CH₄ results in low CH₄ accumulation in the shelf bottom waters even during sulphidic events. Therefore, to understand the major source of CH₄ in the WICS waters and to address the reason behind

the abnormally low CH₄ concentration during sulphidic events, we carried out a systematic experimental study through whole-core incubations over the shelf at two innershelf stations during normoxic and anoxic period to test our hypothesis. We also carried out CH₄-spiked ¹⁵N-labeled incubations in the anoxic subsurface waters to test the occurrence of methanotrophic denitrification i.e. NO₃⁻/NO₂⁻-dependent anaerobic CH₄ oxidation (N-DAMO) which could be responsible for significant anaerobic CH₄ oxidation.

2. Materials and Methods

2.1. Study Area

The Western Indian Continental Shelf (WICS) occupies an area of 310,000 km², of which the inner shelf (Fig. 1) comprises ~33% (Mallik, 2008). The WICS is strongly influenced by the monsoons (the biannual reversal of winds and surface currents) i.e. southwest monsoon during June to September and northeast monsoon during December to February. Southwest monsoon causes moderate upwelling over the shelf during June-September which induces physical, hydrographical and biogeochemical changes in the shelf waters triggering O₂ deficiency (hypoxia) in the subsurface waters (Naqvi et al., 2006). The hypoxia further intensifies into suboxia (O₂<4μM) during July-August and anoxia (O₂=0μM, H₂S>0μM) during September-October (Naqvi et al., 2006) triggering heterotrophic denitrification (Sarkar et al., 2020) and subsequently chemolithoautotrophic (sulphide-driven) denitrification (Pratihary et al., 2023) thereby causing massive N loss. By September, 180,000 km² of the shelf area is covered by low-oxygenated (< 20 μM O₂) waters (Naqvi et al., 2006). The upwelling subsides by late September, and subsequently, with the onset of north-east monsoon during early December, the West India Coastal Current (WICC) reverses its direction by moving poleward (Rao et al., 2008; Shah et al., 2018). This causes downwelling over the shelf leading to vertical mixing and oxygenation of the water column that continues till February (Naqvi et al., 2006). The water column continues to remain well-mixed and oxygenated from March to May as well since the thermal stratification is not observed to be prominent (Naqvi et al., 2006, 2009; Subeesh et al., 2013). The intensity and duration of upwelling and downwelling regimes vary spatially along the shelf (Rao et al., 2008; Shah et al., 2018). The velocity of upwelling has been reported to be 2.77×10⁻² cm s⁻¹ (Unnikrishnan and Antony, 1990) whereas that of downwelling is observed to be 7×10⁻³ cm s⁻¹ (Rao et al., 2008).

2.2. Physico-chemical measurements over the shelf

Physico-chemical measurements were carried out in the shelf water column at 21 stations (Table 1) along the transect off Mumbai, Ratnagiri, Goa, Karwar, Mangalore and Calicut (Fig.1) during

September-October 2011 during the cruise SSK024 on board *RV Sindhu Sankalp*. Further physico-chemical measurements were also done at the station G5 (off Goa) and M1 (off Mangalore) during February 2013 (SSK046 cruise), and again at G5 during October 2013 (SSK056 cruise) and at M1 during October 2024 (SSK176 cruise) onboard *RV Sindhu Sankalp*. Vertical profiles of temperature, salinity and potential density were acquired from a CTD Rosette sampler (Seabird Electronics). Samples for dissolved O₂, H₂S, CH₄ and N-nutrients (NO₃⁻ and NO₂⁻) were collected at discrete depths (0, 9, 18 and 24 m at G5, and 0, 12, 18 and 24 m at M1) using the Rosette sampler at the above stations. O₂ samples (125 mL) were fixed by adding 1 mL of each Winkler's reagent (Grasshoff et al., 1999). H₂S samples (60 mL) were fixed by adding 5 mL of a mixed reagent of N, N-dimethyl-p-phenylenediamine dihydrochloride and FeCl₃ (Grasshoff et al., 1999). CH₄ samples (60 mL) were poisoned by adding 0.3 mL of saturated HgCl₂ solution (Shirodkar et al., 2018). Nutrient samples were kept at 4°C under dark until analysis (Grasshoff et al., 1999).

2.3. CH₄-spiked ¹⁵N-labelled incubations in the water column

During September-October 2011, we carried out CH₄-spiked ¹⁵N-labeled incubation of suboxic/anoxic waters from various depths at stations B2 (off Mumbai), G3, G4, G5 and G6 (off Goa), K3 (off Karwar), M1 and M3 (off Mangalore), C1 (off Calicut) (Fig.1; Table 1) onboard *RV Sindhu Sankalp* (SSK024 cruise) as per the methodology followed by Holtappels et al. (2011) and Steinsdóttir et al. (2022a). Precisely, the samples were collected in 250 mL narrow mouth glass serum bottles by connecting a gas-tight black HDPE tubing (5-6 mm ID) to the nozzle of the Niskin sampler as followed by Holtappels et al (2011). The tubing was flushed sufficiently with sample and squeezed to remove the air bubbles. Then it was inserted into bottom of the serum bottle. The serum bottle was sufficiently flushed with the sample in the same way as O₂ or any gas sample is collected, and then immediately closed with a butyl septa. To release the overpressure, a fine needle was inserted into the septa and the excess water was removed. Then the bottle was immediately crimped. Thereafter, they were purged with zero-grade helium for 20 min to lower the background ²⁸N₂. In one bottle, ¹⁵NO₂⁻ (from 100 mM Na¹⁵NO₂, Sigma-Aldrich) was added to a final concentration of 8 μM, and in the other bottle, ¹⁵NO₂⁻ and CH₄-saturated water (790 μM) were added to the final concentrations of 8 μM and 3 μM, respectively. To prepare the CH₄ saturated water, the water sample from the particular depth was filtered through 0.2 μ mesh. Then the filtered seawater was put into a 250 mL serum bottle and was purged with zero-grade N₂ for 15 minutes and with zero-grade He for another 15 minutes followed by bubbling with 99.97% CH₄ gas standard (Med Gas n Equipment) for 30 minutes with continuous stirring by a magnetic stirrer. Then the CH₄-saturated water was added into the 250 mL serum bottle already enriched with ¹⁵NO₂⁻ so as to obtain a final CH₄ concentration of 3 μM. Then the samples from

the serum bottles were transferred into five 12 mL exetainer vials after sufficient flushing and the vials were quickly capped avoiding any O₂ contamination. Then these vials were incubated at the in-situ temperature for 48 h. At time 0, 12, 24, 36 and 48 h, a 2 mL helium headspace was created in the exetainers, and the samples were poisoned by adding 100 µL of saturated HgCl₂. The headspace samples were analysed for ²⁹N₂ (¹⁴N¹⁵N) and ³⁰N₂ (¹⁵N¹⁵N) by a GC-IRMS (VG Optima) at Max Planck Institute for Marine Microbiology (Germany) within a month.

2.4. Collection of sediment cores

For the whole-core incubation, the shelf sediments were collected at stations G5 (off Goa) and M1 (off Mangalore) during February 2013 (SSK046 cruise), and again at station G5 during October 2013 (SSK056 cruise) and at M1 during October 2024 (SSK176 cruise) (Fig. 1; Table 1) onboard *RV Sindhu Sankalp*, in a box corer from which replicate sediment cores (~22 cm long) were sub-sampled as per Sundbäck et al. (2003), Farias et al. (1996) and Schwartz et al. (2009) in specially-designed cylindrical bevelled Plexiglas core liners (length: 48 cm, ID (inner diameter): 10.1 cm, and thickness: 0.5 cm). During February 2013, six cores were collected at G5 and M1 each. During October, six cores were collected at G5 and four cores were collected at M1. The collected cores were immediately capped at both sides, covered with aluminium foil and brought to a temperature-controlled laboratory onboard. For the measurement of sediment granulometry, porosity and organic carbon at G5 and M1, an additional sediment core were also sub-sampled from the box corer in 6.4 cm ID and 30 cm long bevelled Plexiglas core liners following Baric et al. (2002) and Farias et al (1996). These cores were covered with aluminium foil and kept in the temperature-controlled laboratory.

2.5. Measurement of benthic CH₄ flux by whole-core incubation

The sediment cores were incubated as per the methodology followed by Araujo et al. (2018) and Pratihary et al. (2021). Briefly, the cores were pre-incubated aerobically during February and anaerobically during October for 24 h in order to get them acclimatized to the laboratory condition. During February, the overlying water was continuously oxygenated by introducing air from an aerator. During October, N₂-purged bottom water was put over the sediment cores and they were pre-incubated anaerobically. During both February and October, after 24h of preincubation, the overlying waters in a duplicate set of cores were poisoned by HgCl₂, and the preincubation was continued for another 24 h. After the preincubation, the overlying waters were replaced by freshly collected bottom waters, and the cores were incubated under dark and at temperature close to in-situ temperature in duplicates for 7-9 days under aerobic, anaerobic, and HgCl₂-poisoned conditions during February 2013, and anaerobic, N₂-purged and HgCl₂-poisoned anaerobic (N₂-purged) condition during October 2013

(Suppl. Fig. 1) following the methodologies of Sundbäck et al. (2003), Cornwell et al. (2016), Araujo et al. (2018), and Pratihary et al. (2021). However, during October 2024, cores were incubated under only anaerobic and HgCl₂ poisoned condition in duplicates. In the anaerobic cores (during both February 2013 and October 2013), the overlying water was oxic at time 0 which was allowed to decrease over time. For monitoring of the changes in the water only, the bottom waters were also simultaneously incubated aerobically in 5 L Nalgene polycarbonate (PC) bottles, and anaerobically in 5 L Aluminium-coated gastight trilaminated bags under dark at the in-situ temperature (Suppl. Fig. 1), following Sundbäck et al. (2003), Lehrter et al. (2012), and Cornwell et al. (2014). HgCl₂-added bottom waters were also incubated in 5 L Aluminium-coated gastight trilaminated bags during February and October. A small air headspace was kept in the in the PC bottles and the waters were continuously stirred by a magnetic spindle (Suppl. Fig. 1) while the bags were gently shaken at regular (1 h) interval ensuring proper mixing of the water inside.

Samples for O₂ and CH₄ were collected from the bags, bottles and cores at every 6-12 h intervals. The withdrawn samples in the anaerobic, aerobic and poisoned cores were replaced by the waters from the bags, bottles and bags with poisoned bottom water, respectively during sampling. O₂ samples were collected in a 5 mL Hamilton gastight syringes pre-flushed with helium and were fixed by adding 0.1 mL of each of Winkler's reagents (Pai et al., 1993; Hansen, 1999). The syringes were kept upright in order to allow the oxyhydroxide precipitates to settle. CH₄ samples were collected in 60 mL BD plastic syringes pre-flushed with helium, transferred into 20 mL glass vials after sufficient flushing and poisoned by adding 0.1 mL of saturated HgCl₂ solution. Then the vials were immediately closed with butyl septa without trapping any air bubble, crimped and mixed well.

2.6. Analysis of water and sediment samples

Fixed O₂ samples from various depths were acidified with 1.5 mL of 50% H₂SO₄ solution and measured titrimetrically using a Metrohm titration unit following the method described in Grasshoff et al. (1999), with a precision of ± 1.3 μ M. Fixed O₂ samples from the whole core incubations (including bags and bottles) were acidified with 0.2 mL of 50% H₂SO₄ and the absorbance was measured at 456 nm by a Shimadzu UV-visible spectrophotometer following Pai et al. (1993), with a precision of ± 0.22 μ M. The CH₄ samples were analyzed by a Shimadzu Gas Chromatograph equipped with flame ionization detector, following the multiple headspace extraction method (McAuliffe, 1971; Shirodkar et al., 2018) with a precision of ± 0.2 nM. The absorbance of H₂S samples were measured at 670 nm by a UV-visible spectrophotometer (Grasshoff et al., 1999) with a precision of ± 0.14 μ M. Nutrient samples were thawed to room temperature, mixed well and then colorimetrically analyzed for NO₃⁻ and NO₂⁻ (Grasshoff et al., 1999) by a Skalar segmented flow autoanalyzer, with precisions ± 0.06 μ M

and $\pm 0.006 \mu\text{M}$, respectively. Headspace samples from ^{15}N -labeled incubations were analyzed for $^{14}\text{N}^{15}\text{N}$ ($^{29}\text{N}_2$) and $^{15}\text{N}^{15}\text{N}$ ($^{30}\text{N}_2$) by a GC-IRMS (VG Optima) at Max Planck Institute for Marine Microbiology (Germany) within a month, following the methodology of Holtappels et al. (2011) and Naqvi et al. (2018).

2.7. Analysis of sediment samples

Sediment porosity was determined as per the methodology followed by Pratihary et al. (2014) and Naik et al. (2017). Briefly, the sediment core was sectioned at every 1 cm interval and the slices were weighed. Thereafter, they were oven-dried at 60°C and weighed again to obtain the water content by subtracting the dry weight from the wet weight. Then they were ground and homogenized using an agate mortar and pestle. 2 g of homogenized sediment was taken in a pre-weighed and calibrated 25 ml specific gravity bottle. The bottle was filled with deionized water and mixed well to remove any air bubble entrapped in the sediments. Then the bottle with sediment and water was weighed. The porosity was calculated as per the formula followed by Pratihary et al. (2014). Sedimentary organic carbon (C_{org}) was determined as per the protocol followed by Pratihary et al. (2014, 2021). Briefly, the sediment core was sectioned at 1-2 cm interval, and slices were freeze-dried, homogenized and subsequently decalcified using 1N HCl. C_{org} was measured by IRMS-EA (Delta V plus, Thermo) i.e. an Isotopic Ratio Mass Spectrometer coupled with an Elemental Analyzer with analytical precision $\leq 2\%$. Calibration was done using n-caprioic acid ($\text{C}_6\text{H}_{15}\text{NO}_2$ -ACA) as the laboratory standard as per Higginson and Altabet (2004). Sediment granulometric composition was determined as per the protocol followed by Naik et al. (2017) and Araujo et al. (2018). Briefly, a portion of dried and homogenised sediment slice was weighed and the sand fraction ($<2000 \mu\text{m}$ to $>63 \mu\text{m}$) was separated by sieving the sediment through a $63 \mu\text{m}$ mesh. The silt ($<63 \mu\text{m}$ to $>4 \mu\text{m}$) and clay ($<4 \mu\text{m}$) fractions were analyzed by a Malvern Laser Particle size analyzer (Master size 2000). The percentage of sand, silt and clay were calculated as per Folk (1968).

2.8. Rate calculations and statistical analysis

Linearity of CH_4 concentration (nM) with time (h) was tested through correlation test (MS Excel), and the correlation strength was expressed in terms of r or r^2 . The benthic CH_4 flux rate was calculated only in case of a strong correlation (i.e. $r^2 > 0.85$), following Araujo et al. (2018)) and Pratihary et al. (2021 as follows.

$$F = \frac{V}{A} \times \frac{dC}{dt} \times \frac{24}{1000}$$

where F is the benthic CH_4 flux rate in $\mu\text{mol m}^{-2} \text{d}^{-1}$, V is the volume (in L) of the overlying water in the core, A is the surface area (in m^2) of sediments inside the core, and dC/dt is the slope of the linear regression of CH_4 (in nM) versus time (in hour).

The rate of CH_4 concentration change in the PC bottles (aerobic water systems) and bags (anaerobic water systems) was used to calculate the aerobic and anaerobic production/consumption rate of CH_4 in the water. The aerobic and anaerobic pelagic production/consumption rates (Table 2) were subtracted from production/consumption rate in the aerobic sediment-water and anaerobic sediment-water systems, respectively to obtain the actual benthic CH_4 flux rates (Table 3). As per the conventional denotation, efflux (positive flux) meant flux from the sediment to the water, and influx (negative flux) meant flux from water to sediment.

The denitrification rates in the ^{15}N -labeled incubations were calculated from the linear increase in excess $^{30}\text{N}_2$ production following Thamdrup et al. (2006), Dalsgaard et al. (2012) and Naqvi et al. (2018) as follows.

$$\text{N}_2 \text{ denitrification} = {}^{15}\text{N}^{15}\text{N}_{\text{xs}} \times (F_{\text{NO}_2})^{-2}$$

Where ${}^{15}\text{N}^{15}\text{N}_{\text{xs}}$ is the linear production rate of excess $^{30}\text{N}_2$ (μM) with time (h), and F_{NO_2} is the mole fraction of ^{15}N in the NO_2^- pool in the incubations.

Using Linest function (MS Excel) on the time plot of $^{30}\text{N}_2$, the denitrification rates with standard deviations were calculated (Suppl. Table 1).

To test the significance of the variance between the data sets, single factor ANOVA (MS Excel) was applied, the variance was considered significant only where $p < 0.05$.

3. Results

3.1. Physical and biogeochemical condition over the WICS

The physical and biogeochemical condition of the WICS waters during September-October 2011 has been described in details by Bardhan and Naqvi (2020) and Pratihary et al. (2023). Thermohaline stratification of the water column was observed throughout the shelf with a warm ($25\text{-}29^\circ\text{C}$), low saline (30-33) and oxic surface layer overlying a cold ($21\text{-}23^\circ\text{C}$), high saline (35-35.8) and suboxic/anoxic ($0\text{-}4 \mu\text{M O}_2$) bottom water (Suppl. Fig. 2, 3, 4, 5). The shelf bottom waters were sulphidic ($0.3\text{-}6.4 \mu\text{M H}_2\text{S}$) at stations over Goa (G3, G4, and G5), Mangalore (M1) and Calicut (C1, C2) whereas suboxia ($\text{O}_2 \leq 4 \mu\text{M}$, $\text{NO}_3^- + \text{NO}_2^- > 0 \mu\text{M}$, $\text{H}_2\text{S} = 0 \mu\text{M}$) prevailed at rest of the transects i.e. Mumbai, Ratnagiri and Karwar. Substantial NO_2^- build-up (up to $5.5 \mu\text{M}$) was observed in the suboxic subsurface and bottom waters indicating reductive N loss through microbial denitrification (Naqvi et al., 2006; Sarkar et al.,

2020). Particularly, higher NO_2^- build-up was observed at the suboxic stations (1-5.5 μM) compared to sulfidic stations (0.28-3.6 μM). The shelf water column was observed to be supersaturated with CH_4 at all transects. The surface CH_4 concentration varied from 2.5 to 21.4 nM whereas the bottom CH_4 concentration varied from 3.3 to 36.5 nM. Particularly, surface CH_4 concentrations were higher (5-22.8 nM) at the stations closest to the coast (i.e. B1, R1, G3, K1, M1 and C1) compared to that (2.5-11 nM) at the stations farther from coast, which could be due to the terrestrial run-off (Jayakumar et al., 2001). Overall, higher CH_4 occurred at the surface which gradually decreased downwards up to oxycline and then increased further towards bottom indicating sediments as the source of CH_4 to the water column. However, at most of the stations, although CH_4 increased downwards from oxycline, it further decreased towards bottom indicating anaerobic CH_4 oxidation in the water or sediment.

During February 2013, the water column at both G5 and M1 was well-mixed as the vertical profiles of temperature, salinity and O_2 showed negligible variation from surface to bottom (Fig. 2). No H_2S was observed in the water columns due to the oxygenation of the shelf waters induced by downwelling. CH_4 concentrations were low (<8 nM) at both the stations. However, during October 2013, the water column at both the stations showed thermohaline stratification. A warm (27°C), low saline (34-34.5) and oxic (160-200 μM O_2) surface layer overlaid a cold (22°C), high saline (35) and anoxic (0 μM O_2) subsurface water. Sulphidic condition prevailed at G5 with 0.85 μM H_2S in the bottom water whereas no H_2S was detected in the M1 bottom waters rather it was suboxic. Further observation at M1 during October 2024 (data not shown) showed the biogeochemical condition similar to that during October 2013. At G5, CH_4 concentrations increased downward reaching to 133 nM at the bottom indicating sediments as a CH_4 source. However, at M1, although CH_4 increased downwards to 42 nM at a depth just above the bottom and then decreased towards bottom indicating sediments as a CH_4 sink.

3.2. Sediment characteristics

The solid phase characteristic of the sediments at G5 has already been reported by Naik et al. (2017). Briefly, the sediments at G5 were mainly silt-dominated with depth-averaged composition of 5% sand, 70% silt and 25% clay (Fig. 2). This composition was consistent with that reported by Cowie et al. (2014) over the WICS. The sediment at G5 was found to be highly porous as porosity varied from 0.85 at the surface to 0.78 at 27 cm with an average of 0.8. Sedimentary C_{org} varied from 2.75% at the surface to 2.25% at 27 cm with a mean of 2.34%. However, the sediment solid phase characteristics at M1 (Fig. 2) were observed to be different from that at G5. M1 sediments were found to be sand-dominated with average composition as 62% sand, 30% silt and 8% clay. The porosity varied from 0.36 at the surface to 0.06 at 23 cm with a mean value of 0.16 indicating its less porous nature or higher permeability compared to G5 sediment. Sedimentary C_{org} at M1 varied from 2.23% at the surface to

2.2% at 23 cm with a mean value of 2.12% which was similar to that observed at G5. Top 0.5 cm of the sediment cores at both G5 and M1 appeared pale brown colour below which the sediments looked grey or black as also observed by Pratihary et al. (2014), that was apparently imparted by the Fe- and Mn-oxides (Kurian et al., 2013; Murty and Reddy, 1968) formed due to O₂ penetration into the Fe and Mn-rich sediments of WICS (Naik et al., 2017). The grey or black colour of the underlying sediments was due to the presence of pyrites (Fe sulphides) and Mn sulphides (Naik et al., 2017).

3.3. CH₄ exchange across sediment-water interface

During February, at G5 (off Goa), in the aerobic water systems (PC bottles), O₂ remained >200 µM throughout the incubation indicating sufficient aeration, and CH₄ decreased at the mean rate of 0.137 nM h⁻¹ resulting in the column-integrated pelagic consumption rate of 0.84 µmol m⁻² d⁻¹ indicating its oxidation by O₂ (Fig. 3; Table 2). In the aerobic sediment-water systems (aerobic cores), the O₂ remained >150 µM throughout the incubation, and CH₄ decreased at a mean rate of 0.175 nM h⁻¹ indicating its oxidation by O₂. Conspicuously, the CH₄ consumption rates in the aerobic sediment-water systems were significantly higher than that in the aerobic waters (p=0.02) implying net benthic CH₄ efflux at the mean rate of 0.23 µmol m⁻² d⁻¹. In the anaerobic water systems (bags), O₂ decreased from 266 µM to 43 µM while CH₄ increased from 21 nM up to 41 nM at the rate of 0.095 nM h⁻¹ leading to a column-integrated pelagic production rate of 0.57 µmol m⁻² d⁻¹. However, in the anaerobic sediment-water systems, O₂ decreased substantially from 239 µM to 3.7 µM, and CH₄ increased significantly from 22 nM to 138 nM over ~9 days. The pattern and rate of CH₄ increase in the anaerobic sediment-water systems varied significantly from that in the anaerobic waters (p<0.05). The mean anaerobic benthic CH₄ flux occurred at the rate of 2.55 µmol m⁻² d⁻¹ (Table 3) after deducting pelagic CH₄ production rate (Table 2). In the poisoned sediment-water systems (poisoned cores), O₂ initially decreased to 90 µM but increased thereafter whereas CH₄ significantly increased from 38 nM to 786 nM at the mean flux rate of 25.49 µmol m⁻² d⁻¹. However, no change in O₂ or CH₄ was observed in poisoned water systems i.e. bags (data not shown).

During February, at M1 (off Mangalore), the aerobic water systems showed well oxygenated condition wherein CH₄ increased to 22 nM over 6 days (Fig. 3) at the rate of 0.082 nM h⁻¹ leading to a column-integrated pelagic CH₄ production rate of 0.51 µmol m⁻² d⁻¹ (Table 2). In the aerobic sediment-water systems, the water column remained sufficiently oxic (O₂>214 µM) and CH₄ increased to 30 nM over 5 days indicating CH₄ flux from sediments at a mean rate of 0.37 µmol m⁻² d⁻¹ (Table 3). The pattern of CH₄ increase and benthic CH₄ efflux rates in aerobic sediment-water systems significantly differed from the pattern of CH₄ increase and pelagic CH₄ production rates in the aerobic water systems (p=0.01). In the anaerobic water systems, O₂ decreased up to 127 µM whereas CH₄ increased to 37 nM

at a mean rate of 0.21 nM h^{-1} resulting in a column-integrated pelagic CH_4 production rate of $1.27 \text{ } \mu\text{mol m}^{-2} \text{ d}^{-1}$. In the anaerobic sediment-water systems, O_2 substantially decreased to $18 \text{ } \mu\text{M}$ after 72 h and continued to be low whereas CH_4 linearly increased up to 1840 nM at the mean rate of $74 \text{ } \mu\text{mol m}^{-2} \text{ d}^{-1}$. In the poisoned water systems, no significant change in O_2 or CH_4 was observed (data not shown) whereas in the poisoned sediment-water systems, O_2 decreased up to $127 \text{ } \mu\text{M}$ while CH_4 increased to a very high concentration of 4469 nM (Fig. 3) with a mean flux rate of $152 \text{ } \mu\text{mol m}^{-2} \text{ d}^{-1}$ (Table 3).

During October, at G5, in anaerobic water systems, the initial low O_2 ($25 \text{ } \mu\text{M}$) was quickly consumed leading to euxinia with H_2S build-up after 72 h (Fig. 4). CH_4 increased from time 0 at the rate of 0.106 nM h^{-1} till 72 h and thereafter it decreased at the rate of 0.028 nM h^{-1} which led to an initial column-integrated pelagic CH_4 production rate of $0.62 \text{ } \mu\text{mol m}^{-2} \text{ d}^{-1}$ and subsequently to column-integrated pelagic CH_4 consumption rate of $0.16 \text{ } \mu\text{mol m}^{-2} \text{ d}^{-1}$ (Table 2). The CH_4 production rate in the initial 72 h was not significantly different from that was observed in the anaerobic water during February i.e. $0.57 \text{ } \mu\text{mol m}^{-2} \text{ d}^{-1}$ ($p > 0.05$). CH_4 consumption after 72 h coincided with H_2S build-up. In anaerobic sediment-water systems, O_2 was consumed within 96 h resulting in anoxia whereas CH_4 linearly increased from 27 nM to 101 nM over 9 days (Fig. 4). In the N_2 -purged sediment-water systems, anoxia was established within 12 h and CH_4 linearly increased from 17 nM to 114 nM over 9 days. No significant variance was noticed between the pattern and production rates of CH_4 between anaerobic sediment-water systems and N_2 -purged sediment-water systems ($p > 0.7$). The mean of benthic CH_4 efflux rates from the above two systems (Table 3) was $2.35 \text{ } \mu\text{mol m}^{-2} \text{ d}^{-1}$. In the poisoned water systems, no change in O_2 or CH_4 was noticed (data not shown). In the poisoned sediment-water systems, although O_2 decreased to $21 \text{ } \mu\text{M}$ after 36 h, no significant change was observed after that (Fig. 4). However, CH_4 linearly increased up to a high concentration of 694 nM at a mean benthic flux rate of $22.16 \text{ } \mu\text{mol m}^{-2} \text{ d}^{-1}$ (Table 3).

During October, at M1, in the anaerobic water systems, the initial $16 \text{ } \mu\text{M}$ O_2 decreased to $6 \text{ } \mu\text{M}$ after 6 days. Although CH_4 increased from 3 nM to 11 nM at a linear rate of 0.102 nM h^{-1} particularly after 96 h. In the anaerobic sediment-water systems, O_2 was fully consumed within 72 h whereas CH_4 accumulated up to 1311 nM after 6 days at the mean rate of $75.74 \text{ } \mu\text{mol m}^{-2} \text{ d}^{-1}$. In the poisoned water systems, no change in O_2 or CH_4 was noticed (data not shown). In the poisoned sediment-water systems O_2 remained below $8 \text{ } \mu\text{M}$ with no particular trend in its concentration change. However, CH_4 increased substantially up to $\sim 5 \text{ } \mu\text{M}$ after 10 days at the mean rate of $156.33 \text{ } \mu\text{mol m}^{-2} \text{ d}^{-1}$.

3.4. Denitrification rates with $^{15}\text{NO}_2^-$ and $^{15}\text{NO}_2^- + \text{CH}_4$ amendments

During September-October 2011, in the ^{15}N -labeled incubations, patterns of $^{29}\text{N}_2$ and $^{30}\text{N}_2$ production and the denitrification rates obtained with $^{15}\text{NO}_2^-$ amendment was compared with those obtained with $^{15}\text{NO}_2^- + \text{CH}_4$ amendment (Suppl. Fig. 6-9), and no significant variance was observed ($p > 0.2$). The spatial and vertical variability of the denitrification rate measured with $^{15}\text{NO}_2^-$ has been described in details by Pratihary et al. (2023). Briefly, the denitrification rates with $^{15}\text{NO}_2^-$ amendment varied from 104 to 5573 $\text{nM N}_2 \text{ d}^{-1}$, and that with $^{15}\text{NO}_2^- + \text{CH}_4$ amendment varied from 12 to 5760 $\text{nM N}_2 \text{ d}^{-1}$ at all the stations and depths (Suppl. Table 1; Fig. 5). Notably, the denitrification rates measured with $^{15}\text{NO}_2^- + \text{CH}_4$ amendment did not vary significantly from the corresponding denitrification rates obtained with $^{15}\text{NO}_2^-$ amendment ($p = 0.9$). The denitrification rates were found to be 2-6 times higher at the sulfidic stations (i.e. 221-5573 $\text{nM N}_2 \text{ d}^{-1}$) particularly at the oxic-anoxic interfaces (2079-5573 $\text{nM N}_2 \text{ d}^{-1}$) than the denitrification rates at the suboxic stations (101-901 $\text{nM N}_2 \text{ d}^{-1}$).

4. Discussion

4.1. Benthic CH_4 fluxes during normoxia and anoxia

During February, the aerobic benthic CH_4 flux showed considerable spatial variability in the magnitude and direction, with influx at G5 ($-0.23 \mu\text{mol m}^{-2} \text{ d}^{-1}$) and efflux at M1 ($0.37 \mu\text{mol m}^{-2} \text{ d}^{-1}$). It indicated that CH_4 was consumed by the oxic sediments at G5 while it was released by the oxic sediments at M1. The anaerobic benthic CH_4 flux varied significantly from G5 ($2.55 \mu\text{mol m}^{-2} \text{ d}^{-1}$) to M1 ($74.05 \mu\text{mol m}^{-2} \text{ d}^{-1}$) indicating (a) much higher benthic release under anaerobic than aerobic condition, and (b) spatial variability from north to south. During October, at G5, the anaerobic CH_4 flux rate ($2.35 \mu\text{mol m}^{-2} \text{ d}^{-1}$) was remarkably consistent with that was observed during February considering the standard deviation (Table 3, Fig. 6). Likewise, at M1, the anaerobic CH_4 flux rates were similar during February and October considering the standard deviation (Table 3, Fig. 6). Such consistency of benthic anaerobic CH_4 flux rates between February and October indicated that benthic methanogenesis at both G5 and M1 does not exhibit seasonality. The observed high spatial heterogeneity in benthic CH_4 efflux rate between G5 and M1 could be due to multiple factors e.g. variability in sedimentary organic carbon especially labile carbon, methanogenesis rate, abundance of CH_4 gas pockets and/or sediment granulometric composition between the northern and southern part of the shelf. The mean depth-averaged organic carbon (C_{org}) content of innershelf sediments off Goa is reported to be 2.34% (Naik et al., 2017), while it was 2.12% in the sediments at M1 (Fig. 2). The ratio of protein and carbohydrate to C_{org} (i.e. labile carbon content) of sediments varies from 8.98 at Goa to 8.59 at Mangalore (Jacob et al., 2009). Such statistically insignificant variance in sedimentary

C_{org} and labile C_{org} content between G5 and M1 ($p=0.9$) suggests that the rate of C_{org} -driven methanogenesis possibly does not vary significantly between two sites. However, higher availability of CH_4 gas pockets and/or higher permeability of the sediments at M1 compared to G5 sediments could be the plausible reason of higher benthic CH_4 efflux at M1. Although no data is available yet on the abundance of CH_4 gas pockets at M1, we certainly see a considerable difference in the granulometric composition of sediments between G5 and M1. The sediments at G5 is reported to be composed of 5% sand, 70% silt and 25% clay on an average (Naik et al., 2017) whereas the sediments at M1 contains 62% sand, 30% silt and 8% clay on an average (Fig. 2). Consistently, Jacob et al. (2009) had also observed much higher sand percentage in the innershelf sediments at Mangalore compared to Goa. Moreover, G5 sediment is known to have higher porosity (80%; Naik et al., 2017) compared to 16% porosity of M1 sediments (Fig. 2). This clearly suggested higher permeability of M1 sediments that renders higher mobility to the porewater CH_4 by which it largely escapes the anaerobic oxidation within the sediments and fluxes into the bottom water at much higher rates compared to that at G5.

CH_4 is known to occur at nanomolar levels in the WICS waters (Jayakumar et al., 2001; Shirodkar et al., 2018) whereas the underlying sediments (porewaters) are known to be extremely rich in CH_4 with concentration reaching up to 531 ppm i.e. 33187 μM (Mazumdar et al., 2009). The innershelf sediments of WICS are reported to be CH_4 gas-charged as revealed through high resolution seismic analyses of sediments of 14-47 m-deep stations off Goa (Mazumdar et al., 2009; Dubey and Chaubey et al., 2019). Furthermore, geochemical analysis of these sediments by Mazumdar et al. (2009) confirmed that the CH_4 occurred at concentrations 2.5-4 ppm (156-250 μM) just at the SO_4^{2-} - CH_4 transition zone (2-97 cm) and increased downwards reaching up to 2.7-531 ppm (168-33187 μM) at depths below 1 m with the concomitant downward decrease in SO_4^{2-} concentration. Isotopic analysis showed that these porewater CH_4 are highly depleted in ^{13}C with $\delta^{13}C$ being as low as -88.9 ‰ which indicated the biogenic origin of the CH_4 through CO_2 reduction pathway (Mazumdar et al., 2009). Consistently, another geochemical study of the innershelf sediments off Malvan (150 km north from Goa coast) by Fernandes et al. (2020) corroborated the results of Mazumdar et al. (2009). Several methanogenic archaea e.g. *methanobacteria*, *methanococci*, *methanomicrobia* and *methanopyri* have been reported in the WICS sediments (Bhattacharya et al., 2021), and 50-60% of them belong to *methanosarcinaceae* which can utilize methylated substrates e.g. methanol, methylamines instead of H_2 although many of the methanogenic genera use conventional substrates e.g. H_2 and acetate. The reported high concentration of CH_4 in the sediment porewaters (in μM) and low concentrations in the overlying water column (in nM) is expected to drive extremely high benthic CH_4 efflux as observed in our poisoned sediment-water incubations. However, the observed low aerobic and anaerobic CH_4

efflux rates indicated massive aerobic/anaerobic CH₄ oxidation in the sediments and in the water column.

4.2. Potential benthic CH₄ release and oxidation

Benthic CH₄ efflux rate (mean 23.82 μmol m⁻² d⁻¹) under poisoned condition at G5 was ~10 times higher than the anaerobic CH₄ efflux during both February and October (Table 3, Fig. 6). Similarly, at M1, benthic CH₄ efflux rate under poisoned condition (mean 154.25 μmol m⁻² d⁻¹) was 411 and 2 folds higher than the aerobic and anaerobic CH₄ efflux rates, respectively (Table 3, Fig. 6). Such higher benthic CH₄ effluxes in the poisoned cores compared to the unpoisoned (aerobic and anaerobic) cores were apparently due to complete inhibition of aerobic and anaerobic CH₄ oxidation (methanotrophy) by HgCl₂ not only in the overlying water but also in the sediments. Although CH₄ is produced through methanogenesis in anoxic sediments, a large part of it is unable to flux into the overlying water due to its efficient oxidation within the sediments by various anaerobic bacteria and archaea using oxidants e.g. SO₄²⁻ (Hinrichs et al., 1999; Boetius et al., 2000; Orphan et al., 2001), Mn⁴⁺ and Fe³⁺ (Beal et al., 2009), NO₃⁻ and NO₂⁻ (Raghoebarsing et al., 2006; Ettwig et al., 2008, 2010; Haroon et al., 2013), and also by aerobic bacteria and archaea using O₂ in the top oxic sediments (Boetius and Wenzhöfer, 2013; Lesntra et al. 2023).

Seemingly, in the poisoned aerobic sediment-water systems, penetration of HgCl₂ below the oxic sediment layer not only inhibited the aerobic methanotrophy but also the anaerobic methanotrophy and consequently, CH₄ diffusing from the deeper sediments fluxed into the water up to its full potential without being oxidized. Hence, these CH₄ effluxes can be termed as *potential benthic CH₄ effluxes*, and the difference in potential CH₄ efflux rate and corresponding unpoisoned (aerobic/anaerobic) CH₄ efflux rate can be estimated as the benthic CH₄ oxidation rate (Araujo et al., 2018). Accordingly, the difference between potential benthic CH₄ efflux rate and aerobic (unpoisoned) benthic CH₄ efflux rate can be estimated as *total benthic CH₄ oxidation rate* as it involves both anaerobic and aerobic CH₄ oxidation. However, the difference between potential benthic CH₄ efflux rate and anaerobic (unpoisoned) benthic CH₄ efflux rate can be estimated as the *anaerobic benthic CH₄ oxidation rate* since it involves only anaerobic CH₄ oxidation due to absence of the oxic sediment layer. The difference between total benthic CH₄ oxidation rate and anaerobic benthic CH₄ oxidation rate can be estimated as the *aerobic benthic CH₄ oxidation rate*. Accordingly, during February, the aerobic, anaerobic and total benthic CH₄ oxidation rates were 2.78, 22.94, and 25.49 μmol m² d⁻¹, respectively at G5, and 73.68, 78.13, and 151.81 μmol m² d⁻¹, respectively at M1. However during October, the benthic CH₄ oxidation occurred only anaerobically at the rate of 19.81 μmol m² d⁻¹ at G5, and at the rate of 80.59 μmol m² d⁻¹ at M1.

Considering the prevailing normoxia at G5 and M1 during February, the benthic-produced CH₄ was oxidized within the sediments up to 100 % at G5, and up to 99 % at M1. However, during anoxia, benthic-produced CH₄ was oxidized within the sediments up to 89% at G5, and up to 51% at M1. The rates of benthic anaerobic CH₄ efflux, potential CH₄ efflux and anaerobic CH₄ oxidation at both G5 and M1 were consistent between February and October which suggested that benthic CH₄ release is controlled predominantly by bottom water O₂ regime compared to labile organic carbon. Several anaerobic methanotrophic archaea (ANME) have been detected in the sediments of WICS e.g. *Candidatus Methanoperedens nitroreducens*, *Methanophagales archaeon*, *Methanosarcinales archaeon*, *Methanomicrobiales archaeon*, *ANME-2 cluster archaeon* (Bhattacharya et al., 2021) which were apparently responsible for the observed CH₄ oxidation. The part of CH₄ that escapes the benthic oxidation and fluxes into the water column can get further oxidized in the water column aerobically (Mao et al., 2022; Liu et al., 2024) and anaerobically (Steinsdóttir et al., 2022a, 2022b).

4.3. Pelagic CH₄ production and oxidation

Linear production or consumption of CH₄ in the aerobic and anaerobic water systems clearly indicated that the shelf water itself can be a source or sink of CH₄. During February, at G5, the pelagic CH₄ oxidation rate (0.84 $\mu\text{mol m}^{-2} \text{d}^{-1}$) exceeded the benthic CH₄ oxidation (influx) rate (0.23 $\mu\text{mol m}^{-2} \text{d}^{-1}$) by 3.6 times whereas at M1, the pelagic CH₄ production rate (0.51 $\mu\text{mol m}^{-2} \text{d}^{-1}$) was 1.3 times higher than the benthic CH₄ efflux rate (0.37 $\mu\text{mol m}^{-2} \text{d}^{-1}$) (Table 2, 3). CH₄ is produced in the oxic waters through bacterial cleavage of methylated compounds e.g. methyl phosphonate, methylamine, DMS and DMSP resulting in CH₄-supersaturation of the water (Dam et al., 2010; Florez-Leiva et al., 2013; Karl et al., 2008; Repeta et al., 2016; Wang et al., 2021). In oxic waters, CH₄ is oxidized by O₂ mediated by methane-oxidizing bacteria using O₂-dependent methane monooxygenase gene (Trotsenko and Murrell, 2008). Aerobic CH₄ oxidation (Boetius and Wenzhöfer, 2013; Lenstra et al., 2023) is a significant process which reduces the sea-air CH₄ emission by 50% (Mao et al., 2022). CH₄ was apparently produced and consumed in the shelf waters at both G5 and M1 possibly due to the above mechanisms, and thus, we observed a net pelagic oxidation of CH₄ at G5 and a net pelagic CH₄ production at M1.

During October, at G5, the pelagic CH₄ production rate (0.62 $\mu\text{mol m}^{-2} \text{d}^{-1}$) was very similar ($p < 0.05$) to that in the anaerobic water systems during February (Table 2) despite significant difference in O₂ level in the bags i.e. normoxic/hypoxic during February (Fig. 3) and suboxic/anoxic during October (Fig. 4). A similar rate of pelagic CH₄ production (0.6 $\mu\text{mol m}^{-2} \text{d}^{-1}$) occurred at M1 during October which differed significantly from the anaerobic pelagic CH₄ production rate observed during February (Table 2) indicating anaerobic oxidation of CH₄. Since methanogenesis occurs strictly under anoxic

condition, the observed CH₄ production in non-sulphidic waters appears to be from anoxic microniches rather than from the water. However, the CH₄ consumption just after H₂S build-up (in case of G5) indicated the possible occurrence of anaerobic CH₄ oxidation. A similar trend of CH₄ production under suboxic condition followed by consumption under anoxic condition is speculated at M1 during October if the water would have turned sulphidic. Several past studies over the WICS have reported abnormally low CH₄ build-up in the anoxic/sulphidic bottom waters than in the non-sulphidic (hypoxic/suboxic) or oxic bottom waters (Shirodkar et al., 2018; Gireeshkumar et al., 2017; Sudheesh et al., 2020; Arya et al., 2024). In the WICS bottom waters, CH₄ concentration is not strongly or significantly correlated with H₂S concentration implying no straightforward role of euxinia on the CH₄ build-up (Naqvi et al., 2010; Shirodkar et al., 2018). The southern part of WICS i.e. Mangalore-Kochi is known to experience more intense anoxia with higher H₂S build-up compared to northern part i.e. Mumbai-Goa (Naqvi et al., 2009; Shirodkar et al., 2018), and the CH₄ build-up in the suboxic/anoxic bottom waters is observed to decrease from north to south (Shirodkar et al., 2018). Anoxic/sulphidic shelf waters off Mangalore and Kochi are frequently observed to have 3-7 times lower CH₄ compared to hypoxic or oxic waters in the preceding months (Sudheesh et al., 2020; Arya et al., 2024). A short time-series (36 h) observation of a shallow station off Kochi showed CH₄ decreasing from 200 nM in hypoxic waters to 30 nM in anoxic waters (Arya et al., 2024). Furthermore, CH₄ is also reported to decrease from 400 nM in the oxic waters during April to 50 nM in the anoxic waters during June-September over the shelf (Gireeshkumar et al., 2017). All the above observations clearly indicate significant anaerobic oxidation of CH₄ in the shelf waters during seasonal anoxia and are in agreement with our observation in the bag incubations. Pelagic methanotrophs are known to consume CH₄ to the level below the atmospheric saturation thereby acting as effective CH₄ filters (Reeburgh, 2007), and *Gammaproteobacteria* are considered to be an important pelagic methanotroph in the ocean (Tavormina et al., 2010). Lower CH₄ accumulation under sulphidic condition could also be due to methylation of H₂S resulting in DMS production as observed elsewhere (Lomans et al., 1997; Moran et al., 2008; Li et al. (2023), which warrants further research.

4.4. Fate of benthic-released CH₄ and possibility of N-DAMO (methanotrophic denitrification) in the water column

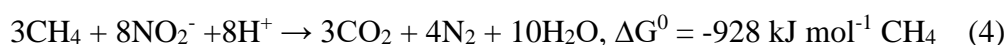
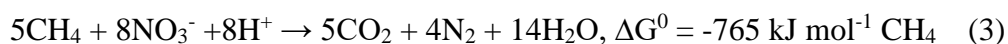
Our whole-core incubation showed that the G5 sediments release CH₄ at the mean rate of 2.45 $\mu\text{mol m}^{-2} \text{d}^{-1}$ during seasonal anoxia which will result in CH₄ accumulation at the rate of 0.16 $\text{nmol L}^{-1} \text{d}^{-1}$ within the suboxic/anoxic subsurface layer (Mean thickness = 15 m) considering the vertical mixing rate of $2.77 \times 10^{-2} \text{ cm s}^{-1}$ due to upwelling over the WICS (Unnikrishnan and Antony, 1990). Along with the mean pelagic CH₄ production rate i.e. 0.1 $\text{nmol L}^{-1} \text{h}^{-1}$ i.e. 2.4 $\text{nmol L}^{-1} \text{d}^{-1}$ (Section 3.2), the

total CH₄ accumulation rate in the water column would be 2.56 nmol L⁻¹ d⁻¹. Likewise, at M1 during October, the CH₄ accumulation rate in the subsurface waters due to the combined effect of benthic (mean) anaerobic flux (74.89 μmol m⁻² d⁻¹) and pelagic production (2.4 nmol L⁻¹ d⁻¹) would be 7.39 nmol L⁻¹ d⁻¹. Reportedly, CH₄ continues to accumulate in the anoxic waters if not interrupted by oxygenation event or anaerobic oxidation (Fenchel et al., 1995; Steinsdóttir et al., 2022a). Thus, considering the CH₄ accumulation in the 15 m-thick suboxic/anoxic subsurface water over 5 month-long seasonal anoxic period (June-October), the CH₄ concentration is expected to reach up to 392 nM corresponding to 18334% saturation at G5, and 1130 nM corresponding to 53248 % saturation at M1. However, the maximum CH₄ concentrations observed in the anoxic subsurface waters at G5 i.e. 133 nM (6220 % saturation) and M1 i.e. 42 nM (1979 % saturation) in our study (Fig. 2) were 3 and 27 times lower than the expected concentrations, respectively, which indicated that the benthic-released and pelagic-produced CH₄ underwent massive anaerobic oxidation in the subsurface waters.

A remarkable correlation between the vertical profile of CH₄ and bottom water O₂ regime (i.e. hypoxic/suboxic/anoxic) was observed over the WICS during September-October 2011 (Suppl. Fig. 10, 11). The stations where the bottom water was hypoxic (i.e. B2, R1, G7 and C3) or anoxic (i.e. G3, G4, G5, M1, C1, C2), the CH₄ showed an increasing trend from the oxycline to the bottom. However, at the stations with suboxic bottom water (i.e. B3, B4, R2, R3, G6, K2, K3, K5, M3, M4), the CH₄ showed an increasing trend from oxycline up to the depth just above the bottom and then showed a significant decrease towards bottom. This pattern in CH₄ profile in response to O₂ regime was also evident during October 2013 (Fig. 2). The former case indicated a net accumulation of CH₄ in the bottom water apparently due to its benthic flux rate exceeding its pelagic oxidation rate, while the latter case indicated net consumption of CH₄ due to its anaerobic oxidation rate exceeding its benthic release rate.

In sediments, methane is known to be anaerobically oxidized by various bacteria and archaea using oxidants e.g. SO₄²⁻ (Hoehler et al., 1994; Boetius et al., 2000; Orphan et al., 2001), Mn⁴⁺ and Fe³⁺ (Beal et al., 2009), NO_x⁻ i.e. NO₃⁻ and/or NO₂⁻ (Raghoebarsing et al., 2006; Ettwig et al., 2008, 2010; Haroon et al., 2013), with NO_x⁻ being the most energetically favourable oxidant among them (Guerrero-Cruz et al., 2021). There are no reports of anaerobic CH₄ oxidation in the water column via SO₄²⁻ reduction (i.e. SO₄²⁻-dependent anaerobic CH₄ oxidation or S-DAMO) or via Mn⁴⁺ and Fe³⁺ reduction (i.e. metal-dependent anaerobic CH₄ oxidation or M-DAMO) so far (Reeburgh, 2007; Knittel and Boetius, 2009; Cui et al., 2015) possibly due to low free energy yield of S-DAMO and low availability of Mn⁴⁺ and Fe³⁺ in the water column. Consequently, this maximizes the possible occurrence of NO_x⁻-dependent anaerobic CH₄ oxidation (N-DAMO) or methanotrophic denitrification

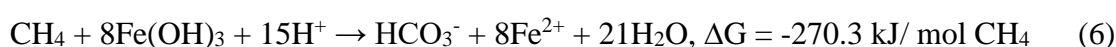
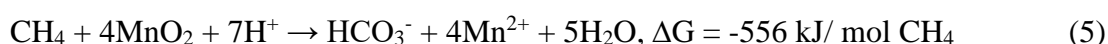
wherein CH₄ oxidation is coupled to NO_x⁻ reduction to N₂ (Eq. 3, 4) mediated by methanotrophic bacteria or archaea (Raghoebarsing et al., 2006; Ettwig et al., 2008, 2010; Haroon et al., 2013). In fact, there are enough geochemical and microbial evidences for the occurrence of N-DAMO in freshwater reservoirs (Naqvi et al., 2018), open ocean OMZs e.g. ETSP (Thamdrup et al., 2019) and semi-enclosed anoxic basins e.g. Mariager Fjord and Golfo Dulce (Steinsdóttir et al., 2022a, 2022b).



The WICS waters are known to be suboxic and replete with NO_x⁻ (mostly NO₂⁻) during late summer monsoon (September) with the average NO₂⁻ concentration of 8 μM (Naqvi et al., 2000, 2006, 2009). Given its high concentration in the suboxic shelf waters, NO_x⁻ (particularly NO₂⁻) can be a potential oxidant of CH₄ in the N-DAMO process. However, we did not observe any significant increase in denitrification rates with the ¹⁵NO₂⁻+CH₄ amendment compared to that with only ¹⁵NO₂⁻ amendment (p=0.9) at any of depths or stations (Suppl. Table 1; Fig. 5) unlike that was observed in the Indian freshwater reservoirs (Naqvi et al., 2018) and ETSP OMZ (Thamdrup et al., 2019). Moreover, the correlation between the denitrification rates and in-situ CH₄ concentrations were poor and insignificant (n=16, r=0.001, p=0.1) (Suppl. Fig. 12). These evidences conspicuously suggested that the benthic-released CH₄ was not oxidized via N-DAMO rather via other alternative processes e.g. M-DAMO or S-DAMO in the suboxic/anoxic subsurface waters over the WICS during seasonal anoxia.

4.5. Other possible processes behind anaerobic CH₄ oxidation

The WICS sediments are known to be Mn-rich (100-870 ppm; Murty et al., 1973; Manjunatha and Shankar, 1997) and Fe-rich (1-7 %; Murty et al., 1973; Naik et al., 2017) with significantly high fraction of reactive Fe i.e. Fe:Al = 0.9-1.4 (Naik et al., 2017). The shelf sediments underlain by suboxic bottom water can experience Mn and Fe reduction. Since M-DAMO is also known to be an energetically favourable process (Eq. 5, 6) in marine sediments (Beal et al., 2009), its occurrence in the suboxic surficial sediments as well as in the bottom waters over the WICS remains a high possibility. In fact, a recent study in the WICS sediments has shown the evidence of anaerobic CH₄ oxidation coupled to Fe- and Mn-reduction (Sivan et al., under review)



CH₄ accumulation in the hypoxic bottom waters at stations B2, R1, G7 and C3 (Suppl. Fig. 10, 11) suggests that the benthic-released CH₄ does not undergo significant anaerobic oxidation at the

sediment-water interface because hypoxia does not trigger Fe and Mn reduction in the surficial sediments and hence results in CH₄ accumulation. However, with the onset of suboxia in the bottom water, Fe and Mn reduction in the surficial sediments oxidizes the previously accumulated CH₄ in the bottom water via M-DAMO, and thus, it leads to lower CH₄ accumulation in the bottom waters compared to the waters at intermediate depths.

After all Fe- and Mn-oxides are reduced in the surficial sediments, bottom water turns sulphidic mainly due to benthic sulphide efflux (Pratihary et al., 2014) that causes sulphidic condition in the WICS bottom waters (Naqvi et al., 2006; Shirodkar et al., 2018) wherein H₂S accumulates up to an average concentration of 5 µM (Pratihary et al., 2023) although it can accumulate up to 15 µM under extreme euxinic events (Naqvi et al., 2000; Shirodkar et al., 2018). Anaerobic CH₄ oxidation coupled to SO₄²⁻ reduction (Martens and Berner, 1977) is carried out through a syntrophic association between anaerobic methanotrophic archaea (ANME) and their partner sulphate-reducing bacteria (SRB) (Hoehler et al., 1994; Boetius et al., 2000; Orphan et al., 2001) through a direct interspecies electron transfer (McGlynn et al., 2015; Wegener et al., 2015).



Within SO₄²⁻-CH₄ transition zone (SMTZ) of marine sediments, S-DAMO has been reported to be more significant than organotrophic SO₄²⁻ reduction (Holmkvist et al., 2011; Jørgensen et al., 2019). In the innershelf sediments off Goa, Naik et al. (2017) observed very high level of H₂S (100-600 µM) but no detectable SO₄²⁻ reduction in the deeper (>12 cm), organic-poor sediments, which indicated that the H₂S was presumably produced in the deeper SMTZ through S-DAMO and diffused upward. In these sediments, Mazumdar et al. (2009) observed the SMTZ at depths 0.7-2.25 m, within which they observed linear downward consumption of porewater SO₄²⁻ and the absence or very low concentration of CH₄ enriched with ¹³C which gave a strong evidence of the occurrence S-DAMO. However, at some shallow sites, SMTZ occurred very close (at 2 cm depth) to the sediment-water interface wherein a high porewater CH₄ (2.5 ppm or 156 µM) was reported (Mazumdar et al., 2009), which increases the possibility of S-DAMO (Eq. 7) occurring in the sulphidic bottom waters as well. During October, the consumption (oxidation) of CH₄ in the G5 waters (in bags) although at a low rate upon the onset of SO₄²⁻ reduction (Fig. 4; Table 2) further gives credence to the possible occurrence of S-DAMO which apparently causes relatively lower CH₄ accumulation in the sulphidic bottom waters as observed by us and reported by Shirodkar et al. (2018) and Sudheesh et al. (2020). However, the consistent accumulation of CH₄ in the sulphidic bottom water and low free energy yield of S-DAMO indicated that S-DAMO is probably not a significant CH₄ consuming process in the anoxic bottom waters of the WICS, compared to M-DAMO that appears energetically more feasible. A future study on

identification and characterization of anaerobic methanotrophic archaea through metagenomics is necessary to confirm the prevalence of various methanotrophic processes over the WICS.

4.6. Comparison with other anoxic coastal systems

A comparative analysis of bottom water CH₄ concentrations and benthic CH₄ flux rates among various shallow anoxic coastal marine systems of world (Table 4) suggests that the bottom water CH₄ concentration of the WICS was one of the lowest, being comparable only to that was reported in Randers Fjord (Abril and Iversen, 2002) and Chilean Shelf (Farias et al., 2021). The benthic CH₄ efflux rate over the WICS is also one of the lowest, being only higher than that was observed in the Baltic Sea (Bonaglia et al., 2017). Naqvi et al. (2010) argued that although higher CH₄ build-up is expected in the anoxic marine waters, deoxygenation is not a necessary and sufficient condition for higher CH₄ accumulation which was evidenced by lack of correlation between H₂S and CH₄ concentration in the WICS waters (Shirodkar et al., 2018). Although, the intensity and frequency of sulphidic event over the WICS are on the rise over last >2 decades (Naqvi et al., 2006, 2009), CH₄ build-up during peak euxinia has been consistently observed to be low (Shirodkar et al., 2018; Sudheesh et al., 2020, Arya et al., 2024) compared to that observed in several other shallow anoxic marine systems (Table 4). This seemingly occurs due to (1) low rate of benthic methanogenesis driven by lower lability of sedimentary organic matter derived from lower pelagic primary production, and (2) high rate of anaerobic benthic CH₄ oxidation over the WICS relative to other shallow anoxic systems wherein higher pelagic productivity leads to higher labile organic content in the sediments and hence higher methanogenesis rate.

4.7. Impact of benthic CH₄ efflux and oxidation on the shelf biogeochemistry

During normoxia, absence of any benthic CH₄ release at G5 and negligibly low benthic CH₄ release at M1 suggested massive aerobic CH₄ oxidation which does not seem to impact the pelagic CH₄ inventory considerably. However, during anoxia, despite high rate of anaerobic benthic CH₄ oxidation, the shelf sediments are able to release CH₄ at modest to high rates which apparently impacts the pelagic CH₄ inventory as evidenced through higher degree of CH₄ super-saturation and consequent higher sea-air CH₄ emission (Shirodkar et al., 2018; Sudheesh et al., 2020). During seasonal anoxia, the potential benthic CH₄ efflux and pelagic methanogenesis suggested that without benthic and pelagic CH₄ oxidation, CH₄ would potentially accumulate in the subsurface waters (15 m thick) at the rate of 3.98 nmol L⁻¹ d⁻¹ at G5 and at the rate of 12.79 nmol L⁻¹ d⁻¹ at M1. Consequently, the CH₄ accumulation in subsurface waters over 5 months of hypoxic-anoxic period (June-October) would result in CH₄ concentrations 609 nM at G5 and 1956 nM at M1, which would correspond to 28,483% and 92172%

CH₄ supersaturation at G5 and M1, respectively. However, the observed low CH₄ concentrations at these stations (i.e. 133 nM at G5 and 42 nM at M1) during October (consistent with the previous observations by Jayakumar et al., 2001; Shirodkar et al., 2018; Sudheesh et al., 2020; Arya et al., 2024) suggested that the benthic and pelagic anaerobic CH₄ oxidation together potentially reduce the water column CH₄ concentration by 4.5 times (by 78%) at G5 and 46 times (by ~98%) at M1. Therefore, the shelf sediments act as an effective methane filter which significantly reduces benthic CH₄ flux to the water column ultimately controlling CH₄ emission to the atmosphere.

Our study showed significant spatial variability in benthic CH₄ efflux rates under both aerobic and anaerobic condition. As discussed in the Section 4.1, the observed spatial variability in anaerobic and potential benthic CH₄ efflux between G5 and M1 could be largely due to the stark difference in granulometric composition of the sediments i.e. silt-clay-dominated sediments at G5 and sand-dominated sediments at M1. In terms of sediment mineralogy and geochemistry, a clear provinciality has been observed between the shelf north of Goa (15°N) and south of Goa (Rao and Rao, 1995; Kurian et al., 2013). In fact, Jacob et al. (2009) observed a considerable difference in granulometric composition of the sediments of northern section (i.e. north of 15° N) and southern section (i.e. south of 15° N) of the innershelf wherein the sediments between 15°-21° N were largely silty-clayey (72-95% silt, 4-27% clay and <0.2-4% sand), and the sediments between 9°-13°N were largely sandy (28-83% sand, <0.2-51% silt and 9-20% clay). High resolution seismic reflection studies have revealed widespread occurrence of methane gas-charged sediments from Gulf of Kachchh to Cochin covering almost the entire innershelf of Western India (Karisiddaiah and Veeraya, 1994). This implies the occurrence of benthic CH₄ efflux and CH₄ oxidation over the entire innershelf although with spatial variability. Given the contrasting sediment granulometry between northern and southern shelf, G5 and M1 can be considered as the representative of northern and southern innershelf, respectively. The total area of the innershelf is 102,300 Km² (Mallik, 2008), of which the northern and southern section occupies ~50% of area each. Considering the mean anaerobic benthic CH₄ efflux rate and mean potential benthic CH₄ efflux rate observed during February and October, and the area-integrated benthic CH₄ efflux rates and potential benthic CH₄ efflux rates over northern and southern shelves, the total annual benthic CH₄ efflux and potential benthic CH₄ efflux rate from the entire shelf were 9.45 Gg y⁻¹ and 53.71 Gg y⁻¹, respectively, and the total annual benthic CH₄ oxidation rate was 30.71 Gg y⁻¹.

5. Conclusions

Whole-core incubations over the innershelf off Western India showed that the sediments are negligible CH₄ source or sink during normoxia and a low to moderate CH₄ source to the water column during

anoxia. Aerobic and anaerobic methanotrophy within the sediments consumes 51-100 % of CH₄ produced through methanogenesis and thus play a crucial role in controlling the benthic CH₄ release to the water column. During seasonal anoxia, the benthic-released CH₄ undergoes further anaerobic oxidation in the water column, not via NO_x⁻ reduction (N-DAMO) but rather possibly via Fe- and Mn-oxide reduction and/or SO₄²⁻ reduction which substantially reduces the CH₄ accumulation in the anoxic shelf waters. Without benthic and pelagic methanotrophy, the pelagic CH₄ supersaturation would potentially reach up to 92172 % which would ultimately result in much higher CH₄ emission from the shelf. Thus, the Western Indian shelf acts as effective benthic methane filter which ultimately minimizes CH₄ emission to the atmosphere.

Acknowledgements

The authors gratefully acknowledge Dr. S.W.A. Naqvi, the erstwhile Director of CSIR-National Institute of Oceanography (NIO), for helping with the methodology and ¹⁵N-N₂ measurement related to N-DAMO process, and providing laboratory and logistic facilities for the benthic flux measurements. We sincerely thank Dr. Marcel Kuypers and Dr. Gaute Lavik for providing the laboratory facility for the ¹⁵N-N₂ measurement by GC-IRMS at the Max Planck Institute for Marine Microbiology (MPIMM). AP gratefully acknowledges German Academic Exchange Service (DAAD) for providing the Post-doctoral Scholarship (A/09/74775) and funding the research work related to N-DAMO. We thank Anand Methar for processing the CTD data, and designing the experimental set up for the benthic flux measurement. We thank Dr. Siby Kurian and Kausar Bepari for their assistance in the ¹⁵N-incubations and core incubations, respectively. We thank Dr. Hema Uskaikar for providing some biogeochemical data used in this manuscript. We thank the Captain and crews of *RV Sindhu Sankalp*, and Ship cell staffs Siddharth Vernekar, Shashikant Velip, Buddhadas Patole and Kallathian M. for their kind help and technical assistance during SSK024, SSK046, SSK056 and SSK176 cruises. The research work related to benthic flux was funded by Ministry of Earth Sciences (MoES), Govt. of India, through SIBER India projects GAP 2424 and GAP 2425, and Deep Ocean Mission project GAP3631. This is CSIR-NIO contribution no. xxxx.

References

- Abril, G., Iversen, N., 2002. Methane dynamics in a shallow non-tidal estuary (Randers Fjord, Denmark). *Mar. Ecol. Prog. Ser.* 230, 171-181.
- Araujo, J., Naqvi, S.W.A., Naik, R., Naik, H., 2018. Biogeochemistry of methane in a tropical monsoonal estuarine system along the west coast of India. *Estuar. Coast. Shelf Sci.* 207, 435–443.

- Arx, J.N., Kidane, A.T., Philippi, M., Mohr, W., Lavik, G., Schorn, S., Kuypers, M.M.M., Milucka, J., 2023. Methylphosphonate-driven methane formation and its link to primary formation and its link to primary production in the oligotrophic North Atlantic. *Nat. Comm.* 14, 6529.
- Arya, K.S., Gireeshkumar, T.R., Vignesh, E.R., Muraleedharan, K.R., Jaleel, K.U.A., Razaque, M.A.A., Furtado, C.M., Sudheesh, V., Nair, T.M.B., Krishnamohan, K.S., 2024. Dynamics of nitrous oxide and methane in the southeastern Arabian Sea. *Mar. Chem.* 258, 104333.
- Bardhan, P., Naqvi, S.W.A., 2020. Nitrogen and carbon cycling over the western continental shelf of India during seasonal anoxia: A stable isotope approach. *J. Mar. Syst.* 207, 103144.
- Baric, A., Kuspilic, G., Matijevik, S., 2002. Nutrient (N, P, Si) fluxes between marine sediments and water column in coastal and open Adriatic. *Hydrobiol.* 475/476, 151-159.
- Beal, E.J., House, C.H., Orphan, V.J., 2009. Manganese- and iron-dependent marine methane oxidation. *Science* 325, 184-187.
- Bhattacharya, S., Mapdar, T., Fernandes, S., Roy, C., Sarkar, J., Rameez, M.J., Mandal, S., Sar, A., Chakraborty, A.K., Mondal, N., Chatterjee, S., Dam, B., Peketi, A., Chakraborty, Mazumdar, A., Ghosh, W., 2021. Sedimentation rate and organic matter dynamics shape microbiome across a continental margin. *Biogeosciences*, 18, 5203-5222.
- Boetius, A., Ravensschlag, K., Schubert, C.J., Rickert, D., Widdel, F., Gieseke, A., Amann, R., Jorgensen, B.B., Witte, U., Pfannkuche, O., 2000. A marine microbial consortium apparently mediating anaerobic oxidation of methane. *Nature* 407, 623-626.
- Boetius, A., Wenzhöfer, F., 2013. Seafloor oxygen consumption fuelled by methane from cold seeps. *Nat. Geoscience* 6, 725-734.
- Bonaglia, S., Brüchert, V., Callac, N., Vicenzi, A., Fru, E.C., Nascimento, F.J.A., 2017. Methane fluxes from coastal sediments are enhanced by macrofauna. *Sci. Rep.* 7, 13145.
- Bonaglia, S., Rütting, T., Kononets, M., Stigebrandt, A., Santos, I.R., Hall, P.O.J., 2022. High methane emissions from an anoxic fjord driven by mixing and oxygenation. *Limnol. Oceanogr. Lett.* 7, 392-400.
- Borges, A.V., Champenois, W., Gypens, N., Delille, B., Harlay, J., 2016. Massive methane emissions from near-shore shallow coastal areas. *Sci. Rep.* 6: 27908.
- Brüchert, V., Currie, B., Peard, K.R., 2009. Hydrogen sulphide and methane emissions on the central Namibian shelf. *Prog. Oceanogr.* 83, 169-179.
- Capelle, D. W., Hallam, S. J., Tortell P. D., 2019. Time series CH₄ measurements from Saanich inlet, BC, a seasonally anoxic fjord. *Mar. Chem.* 215, 103664.
- Farias, L., Tenerio, S., Sanzana, K., Faundez, J., 2021. Temporal methane variability in the water column of an area of seasonal coastal upwelling: A study based on a 12 year time series. *Prog. Oceanogr.* 195, 102589.
- Cornwell, J.C., Glibert, P.M., Owens, M.S., 2014. Nutrient fluxes from sediments in the San Francisco Bay delta. *Estuar. Coast* 37, 1120-1133.

- Cornwell, J.C., Owens, M.S., Boynton, W.R., Harris, L.A., 2016. Sediment-water nitrogen exchange along the Potomac River estuarine salinity gradient. *J. Coast. Res.* 32 (4), 776–787.
- Cowie, G., Mowbray, S., Kurian, S., Sarkar, A., White, C., Anderson, A., Vergnaud, B., Johnstone, G., Brear, S., Woulds, C., Naqvi, S.W.A., Kitazato, H., 2014. Comparative organic geochemistry of Indian margin (Arabian Sea) sediments: estuary to continental slope. *Biogeosciences*, 11, 6683-6696.
- Crutzen, P.J., Zimmermann, P.H., 1991. The changing photochemistry of the troposphere. *Tellus* 43AB, 136-151.
- Dalsgaard, T., Thamdrup, B., Farias, L., Revsbech, N.P., 2012. Anammox and denitrification in the oxygen minimum zone of the eastern South Pacific. *Limnol. Oceanogr.* 57 (5), 1331–1346.
- Damm, E., Helmke, E., Thoms, S., Schauer, U., Nöthig, Bakker, K., Kiene, R.P., 2010. Methane production in aerobic oligotrophic surface surface waters in the central Arctic Ocean. *Biogeosciences* 7, 1099-1108.
- DelSontro, T., Beaulieu, J.J., Downing, J.A., 2018. Greenhouse gas emissions from lakes and impoundments: Upscaling in the face of global change. *Limnol. Oceanogr. Lett.* 3, 64-75.
- Dlugokencky, E.J., Walter, B.P., Masarie, K.A., Lang, P.M., Kasischke, E.S., 2001. Measurements of an anomalous global methane increase during 1998. *Geophys. Res. Lett.* 28, 499-502.
- Dubey, K.M., Chaubey, A.K., 2019. Origin and distribution of shallow gas-charged sediment on the inner continental shelf of central west coast of India. *Curr. Sci.* 116 (8), 1410-1417.
- Ettwig, K.F., Shima, S., van de Pas-Schoonen, K.T., Kahnt, J., Medema, M.H., Op den Camp, H.J., Jetten M.S.M., Strous, M., 2008. Denitrifying bacteria anaerobically oxidize in the absence of archaea. *Environ. Microbiol.* 10 (11), 3164-3173.
- Ettwig, K.F., Butler, M.K., Le Paslier, D. Et al., 2010. Nitrite-driven anaerobic methane oxidation by oxygenic bacteria. *Nature* 464, 543-549.
- Farias, L., Chuecas, L.A., Salamanca, M.A., 1996. Effect of coastal upwelling on nitrogen regeneration from sediments and ammonium supply to the water column in Concepcion Bay, Chile. *Estuar. Coast. Shelf Sci.* 43, 137-155.
- Farias, L., Tenorio, S., Sanzana, K., Faundez, J., 2021. Temporal methane variability in the water column of an area of seasonal coastal upwelling: A study based on a 12 year time series. *Prog. Oceanogr.* 195, 102589.
- Fenchel, T., Bernard, C., Esteban, G., Finlay, B. J., Hansen, P. J., Iversen, N., 1995. Microbial diversity and activity in a Danish fjord with anoxic deep water. *Ophelia* 43, 45–10.
- Fernandes, S., Mazumdar, A., Peketi, A., Anand, S.S., Rengarajan, R., Jose, A., Manaskanya, A., Carvalho, M.A., Shetty, D., 2020. Sulfidization processes in seasonally hypoxic shelf sediments: A study off the West coast of India. *Mar. Petr. Geol.* 117, 104353.
- Florez-Leiva, L., Damm, E., Farías, L., 2013. Methane production induced by dimethylsulfide in surface water of an upwelling ecosystem. *Prog. Oceanogr.* 112-113, 38-48.

- Folk, R.L., 1968. Petrology of Sedimentary Rocks. Hemphills, Drawer's M. University Station, Austin, Texas, pp. 170.
- Garcia, J.L., Patel, B.K.C., Ollivier, B., 2000. Taxonomic, Phylogenetic, and ecological diversity of methanogenic archaea. *Anaerobe* 6, 205-226.
- Gireeshkumar, T.R., Mathew, D., Pratihary, A.K., Naik, H., Narvekar, K.U., Araujo, J., Balachandran, K.K., Muraleedharan, K.R., Thorat, B., Nair, M., Naqvi, S.W.A., 2017. Influence of upwelling induced near shore hypoxia on the Alappuzha mud banks, South west coast of India. *Cont. Shelf Res.* 139, 1-8.
- Grasshoff, K., Kremling, K., Ehrhardt, M., 1999. *Methods of Seawater Analysis*, 3rd ed. Wiley-VCH Verlag GmbH.
- Guerrero-Cruz, S., Vaksmaa, A., Horn, M.A., Niemann, H., Pijuan, M., Ho, A., 2021. Methanotrophs: Discoveries, environmental relevance, and a perspective on current and future applications. *Front. Microbiol.* 12, 678057. Doi: 10.3389/fmicb.2021.678057.
- Gülzow, W., Rehder, G., Deimling, J.S., Seifert, T., Tóth, Z., 2013. One year of continuous measurements constraining methane emissions from the Baltic Sea to the atmosphere using a ship of opportunity. *Biogeosciences* 10, 81-99.
- Hansen, H.P., 1999. Determination of oxygen. In: Grasshoff, K., Kremling, K., Ehrhardt, M. (Eds.), *Methods of Seawater Analysis*. Wiley-VCH, Berlin, pp. 75–88.
- Haroon, M.F., Hu, S., Shi, Y., Imelfort, M., Keller, J., Hugenholtz, P., Yuan, Z., Tyson, G.W., 2013. Anaerobic oxidation of methane coupled to nitrate reduction in a novel archaeal lineage. *Nature* 500, 567-570.
- Hinrichs, K., Hayes, J.M., Sylva, S.P., Brewer, P.G., DeLong, E.F., 1999. Methane-consuming archaeobacteria in marine sediments. *Nature* 398, 802-805.
- Higginson, M.J., Altabet, M.A., 2004. Comment on ‘Sedimentary phosphorus record from the Oman margin: new evidence of high productivity during glacial periods’, by F. Tamburini et al. *Paleoceanography* 19, PA2024, doi:10.1029/2004PA001017.
- Hoehler, T. M., Alperin, M. J., Albert, D. B., Martens, C. S., 1994. Field and laboratory studies of methane oxidation in an anoxic marine sediment: evidence for a methanogen-sulfate reducer consortium. *Global Biogeochem. Cy.* 8, 451–463.
- Holtappels, M., Lavik, G., Jensen, M.M., Kuypers, M.M.M., 2011. 15N-Labeling experiments to dissect the contributions of heterotrophic denitrification and anammox to nitrogen removal in the OMZ waters of the ocean. *Methods Enzymol.* 486, 223–251.
- Holmkvist, L., Ferdelman, T.G., Jørgensen, B.B., 2011. A cryptic sulfur cycle driven by iron in the methane zone of marine sediment (Aarhus Bay, Denmark). *Geochim. Cosmochim. Acta.* 75, 3581-3599.
- Jacob, J., Jayaraj, K.A., Rehman, H.H., Chandramohanakumar, N., Balachandran, K.K., Raveendran, T.V., Joseph, T., Nair, M., Achuthankutty, C.T., 2009. Biogeochemical characteristics of the surface sediments along the western continental shelf of India. *Chem. Ecol.* 25 (2), 135-149.

- Jayakumar, D.A., Naqvi, S.W.A., Narvekar, P.V., George, M.D., 2001. Methane in coastal and offshore waters of the Arabian Sea. *Marine Chemistry* 74, 1-13.
- Jørgensen, B.B., Beulig, F., Egger, E., Petro, C., Scholze, C., Roy, H., 2019. Organoclastic sulfate reduction in the sulfate-methane transition of marine sediments. *Geochim. Cosmochim. Acta.* 254, 231-245.
- Karisiddaiah, S.M., Veerayya, M., 1994. Methane-bearing shallow gas-charged sediments in the eastern Arabian Sea: a probable source for greenhouse gas. *Cont. Shelf. Res.* 12, 1361-1370.
- Karl, D.M., Beversdorf, L., Björkman, K.M., Church, M.J., Martinez, A., Delong, E.F., 2008. Aerobic production of methane in the sea. *Nat. Geosci.* 1, 473-478.
- Ketzer, M., Stranne, C., Rahmati-Abkenar, M., Shahabi-Ghahafarokhi, S., Jaeger, L., Pivel, M.A.G., Josefsson, S., Zillén, L., 2024. Near seafloor methane flux in the world's largest human-induced dead zone is regulated by sediment accumulation rate. *Mar. Geol.* 468, 107220.
- Klitzsch, T., Geisinger, H., Wieland, A., Langer, G., Nehrke, G., Bizic, M., Greule, M., Lenhart, K., Borsch, C., Schroll, M., Keppler, F., 2023. Stable carbon isotope signature of methane released from phytoplankton. *Geophys. Res. Lett.* 50, e2023GL103317.
- Kurian, S., Nath, B.N., Kumar, N.C., Nair, K.K.C., 2013. Geochemical and isotopic signatures of surficial sediments from the Western continental shelf of India: Inerring provenance, weathering, and the nature of organic matter. *J. Sed. Res.* 83, 427-442.
- Lehrter, J.C., Beddick Jr., D.L., Devereux, R., Yates, D.F., Murrell, M.C., 2012. Sediment-water fluxes of dissolved inorganic carbon, O₂, nutrients, and N₂ from the hypoxic region of the Louisiana continental shelf. *Biogeochem.* 109, 233-252.
- Lenstra, W.K., van Helmond, N.A.G.M., Martins, P.D., Wallenius, A.J., Jetten, M.S.M., Slomp, C.P., 2023. Gene-based modelling of methane oxidation in coastal sediments: Constraints on the efficiency of the microbial methane filter. *Environ. Sci. Technol.* 57, 12722-12731.
- Liu, Q., Du, G., Li, X., Liu, J., Meng, N., Li, C., Liu, X., Zhang, G., Yang, G., Joye, S., Zhuang, G., 2024. Dynamics and controls of methane oxidation in the aerobic waters of Eastern China marginal seas. *J. Geophys. Res.: Oceans*, 129, e2023JC020280.
- Li, C., Cao, H., Wang, Q., Carrión, O., Zhu, X., Miao, J., Wang, P., Chen, X., Todd, J.d., Zhang, Y., 2023. Aerobic methylation of hydrogen sulfide to dimethylsulfide in diverse microorganisms and environments. *ISME J.* 17, 1184-1193.
- Lomans, B.P., Smolders, A.J.P., Intven, L.M., Pol, A., den Camp, H.J.M.O., van der Drift, C., 1997. Formation of dimethyl sulfide and methanethiol in anoxic freshwater sediments. *Appl. Environ. Microbiol.* 63 (12), 4741-4747.
- Mallik, T. K.: *Marine Geology: A scenario around Indian coasts*, New Academic Publishers, 457 pp., 2008.
- Mao, S., Zhang, H., Zhuang, G., Li, X., Liu, Q., Zhou, Z., Wang, W., Li, C., Lu, K., Liu, X., Montgomery, A., Joye, S.B., Zhang Y., Yang, G., 2022. Aerobic oxidation of methane significantly reduces global diffusive methane emissions from shallow marine waters. *Nat. Comm.* 13: 7309.

- Mazumdar, A., Peketi, A., Dewangan, P., Badesab, F., Ramprasad, T., Ramana, M.V., 2009. Shallow gas charged sediments off the Indian west coast: Genesis and distribution. *Mar. Geol.* 267, 71-85.
- McAuliffe, C., 1971. GC determination of solutes by multiple phase equilibration. *Chem. Tech.* 1, 46–50.
- McGlynn S.E., Chadwick, G.L., Kempes, C.P., Orphan, V.J., 2015. Single cell activity reveals direct electron transfer in methanotrophic consortia. *Nature* 526, 531–535.
- Moran, J.J., House, C.H., Vrentas, J.M., Freeman, K.H., 2008. Methyl sulfide production by a novel carbon monoxide metabolism in *Methanosarcina acetivorans*. *Appl. Environ. Microbiol.* 74 (2), 540-542.
- Naik, R., Naqvi, S.W.A., Araujo, J., 2017. Anaerobic carbon mineralisation through sulphate reduction in the inner shelf sediments of eastern Arabian Sea. *Estuar. Coast.* 40, 134-144.
- Murty, P.S.N., Rao, C.M., Reddy, C.V.G., 1973. Partition patterns of iron, manganese, nickel and cobalt in the shelf sediments off West coast of India. *Ind. J. Mar. Sci.* 2, 6-12.
- Naqvi, S.W.A., Jayakumar, D.A., Narvekar, P.V., Naik, H., Sarma, V.V.S.S., D'Souza, W., Joseph, S., George, M.D., 2000. Increased marine production of N₂O due to intensifying anoxia on the Indian continental shelf. *Nature* 408, 346–349.
- Naqvi, S. W. A., H. Naik, D. A. Jayakumar, M. S. Shailaja, and P. V. Narvekar. 2006. Seasonal oxygen deficiency over the western continental shelf of India, p. 195–224. In L. N. Neretin [ed.], *Past and Present Water Column Anoxia*. Springer.
- Naqvi, S.W.A., Bange, H.W., Farías, L., Monteiro, P.M.S., Scranton, M.I., Zhang, J., 2010. Marine hypoxia/anoxia as a source of CH₄ and N₂O. *Biogeosciences* 7, 2159-2190.
- Naqvi, S.W.A., Lam, P., Narvenkar, G., Sarkar, A., Naik, H., Pratihary, A., Shenoy, D.M., Gauns, M., Kurian, S., Damare, S., Duret, M., Lavik, G., Kuypers, M.M.M., 2018. Methane stimulates massive nitrogen loss from freshwater reservoirs in India. *Nat. Comm.* 9, 1265.
- Orphan, V.J., Hinrichs, K.U., Ussler III, W., Paull, C.K., Taylor, L.T., Sylva, S.P., Hayes, J.M., Delong, E.F., 2001. Comparative analysis of methane-oxidizing archaea and sulfate-reducing bacteria in anoxic marine sediments. *Appl. Environ. Microbiol.* 67 (4), 1922-1934.
- Owens, M.S., Cornwell, J.C., 2016. The benthic exchange of O₂, N₂ and dissolved nutrients using small core incubations. *J. Visual. Exp.* 114, e54098. doi:10.3791/54098.
- Pai, S., Gong, G., Liu, K., 1993. Determination of dissolved oxygen in seawater by direct spectrophotometry of total iodine. *Mar. Chem.* 41, 343–351.
- Pratihary, A.K., Naqvi, S.W.A., Narvenkar, G., Kurian, S., Naik, H., Naik, R., Manjunatha, B.R., 2014. Benthic mineralization and nutrient exchange over the inner continental shelf of western India. *Biogeosciences.* 11 (10), 2771–2791.
- Pratihary, A., Naik, R., Karapurkar, S., Gauthankar, M., Khandeparker, R., Manjrekar, S., Gauns, M., 2021. Benthic exchange along a tropical estuarine salinity gradient during dry season: Biogeochemical and ecological implications. *J. Sea Res.* 177, 102124.

- Pratihary, A.K., Lavik, G., Naqvi, S.W.A., Shirodkar, G., Sarkar, A., Marchant, H., Ohde, T., Shenoy, D., Kurian, S., Uskaikar, H., Kuypers, M.M.M., 2023. Chemolithoautotrophic denitrification intensifies nitrogen loss in the Eastern Arabian Sea Shelf waters during sulphidic events. *Prog. Oceanogr.* 217, 103075.
- Raghoebarsing, A., Pol, A., van de Pas-Schoonen, K.T., Smolders, A.J.P., Ettwig, K.F., Rijpstra, W.I.C., Schouten S., Damsté, J.S.S., Op den Camp, H.J., Jetten M.S.M., Strous, M., 2006. A microbial consortium couples anaerobic methane oxidation to denitrification. *Nature* 440, 918-921.
- Rao, A.D., Joshi, M., Ravichandran, M., 2008. Oceanic upwelling and downwelling processes off the west coast of India. *Ocean Dyn.* 58, 213-226.
- Rao, V.P., Rao, B.R., 1995. Provenance and distribution of clay minerals in the sediments of western continental shelf and slope of India. *Cont. Shelf. Res.* 15 (14), 1757-1771.
- Reeburgh, W.S., 2007. Oceanic methane biogeochemistry. *Chem. Rev.* 107, 486-513.
- Repeta, D.J., Ferron, S., Sosa, O.A., Johnson, C.G., Repeta, L.D., Acker, M., Delong, E.F., Karl, D.M., 2016. Marine methane paradox explained by bacterial degradation of dissolved organic matter. *Nat. Geosci.* 9, 884-890.
- Sarkar, A., Naqvi, S.W.A., Lavik, G., Pratihary, A., Naik, H., Shirodkar, G., Kuypers, M.M.M., 2020. Massive nitrogen loss over the Western Indian Continental Shelf during seasonal anoxia: Evidence from isotope pairing technique. *Front. Mar. Sci.* 7: 678. Doi:10.3389/fmars.2020.00678.
- Saunois, M., Stavert, A.R., Poulter, B. et al., 2020. The global methane budget 2000-2007. *Earth Syst. Sci. Data*, 12, 1561-1623.
- Schwartz, M.C., Woulds, C., Cowie, G.L., 2009. Sedimentary denitrification rates across the Arabian Sea oxygen minimum zone. *Deep-Sea Res. II* 56, 324-332.
- Shah, P., Sajeev, R., Santhosh, K.M., Thara, K.J., Shafeeque, M., John, K.L., George, G., 2018. Observed signals of upwelling and downwelling along the west coast of India. *Ind. J. Geo Mar. Sci.* 47 (03), 604-612.
- Shenoi, S., Antony, M.K., 1991. Current measurements over the western continental shelf of India. *Cont. Shelf Res.* 11 (1), 81-93.
- Shirodkar, G., Naqvi, S.W.A., Naik, H., Pratihary, A.K., Kurian, S., Shenoy, D.M., 2018. Methane dynamics in the shelf waters of the West coast of India during seasonal anoxia. *Mar. Chem.* 203, 55-63.
- Sivan, K., Peketi, A., Mazumdar, A., Zatale, A., Pillutla, S.P.K., Ghosh, A., Sadique, M., Mathai, J., Enigmatic Fe-Mn-fueled anaerobic oxidation of methane in sulfidic coastal sediments of the Eastern Arabian Sea. Under review in *EGU sphere*, <https://doi.org/10.5194/egusphere-2024-1829>
- Steinle, L., Maltby, J., Treude, T., Kock, A., Bange, H.W., Engbersen, N., Zopfi, J., Lehmann, M.F., Niemann, H., 2017. Effects of low oxygen concentrations on aerobic methane oxidation in seasonally hypoxic coastal waters. *Biogeosciences* 14, 1631-1645.
- Steinsdóttir, H.G.R., Schauburger, C., Mhatre, S., Thamdrup, B., Bristow, L.A., 2022. Aerobic and anaerobic methane oxidation in a seasonally anoxic basin. *Limnol. Oceanogr.* 1999, 1-17.

- Steinsdóttir, H.G.R., Gomez-Ramírez, E., Mhatre, S., Schaubberger, C., Bertagnolli, A.D., Pratte, Z.A., Stewart, F.J., Thamdrup, B., Bristow, L.A., 2022. Anaerobic methane oxidation in a coastal oxygen minimum zone: spatial and temporal dynamics. *Environ. Microbiol.* 24 (5), 2361-2379.
- Subeesh, M.P., Unnikrishnan, A.S., Fernando, V., Agarwadekar, Y., Khalap, S.T., Satelkar, N.P., Shenoi, S.S.C., 2013. Observed tidal currents on the continental shelf off the west coast of India. *Cont. Shelf Res.* 69, 123-140.
- Sudheesh, V., Gupta, G.V.M., Naqvi, S.W.A., 2020. Massive methane loss during seasonal hypoxia/anoxia in the nearshore waters of Southeastern Arabian Sea. *Front. Mar. Sci.* 7:324, doi:10.3389/fmars.2020.00324.
- Sundbäck, K., Miles, A., Hulth, S., Pihl, L., Engström, P., Selander, E., Svenson, A., 2003. Importance of benthic nutrient regeneration during initiation of macroalgal blooms in shallow bays. *Mar. Ecol. Prog. Ser.* 246, 115–126.
- Tavormina, P.L., Ussler III, W., Joye, S.B., Harrison, B.K., Orphan, V.J., 2010. Distributions of putative aerobic methanotrophs in diverse pelagic marine environments. *The ISME J.* 4, 700-710.
- Thamdrup, B., Dalsgaard, T., Jensen, M.M., Ulloa, O., Farias, L., Escribano, R., 2006. Anaerobic ammonium oxidation in the oxygen-deficient waters off northern Chile. *Limnol. Oceanogr.* 51 (5), 2145–2156.
- Thamdrup, B., Steinsdottir, H. G. R., Bertagnolli, A. D., Padilla, C. C., Patin, N. V., Garcia-Robledo, E., Bristow, L. A., Stewart, F. J., 2019. Anaerobic methane oxidation is an important sink for methane in the ocean's largest oxygen minimum zone. *Limnol. Oceanogr.* 64, 2569–2585.
- Thauer, R.K., Kaster, A.K., Seedorf, H., Buckel, W., Hedderich, R., 2008. Methanogenic archaea: ecologically relevant differences in energy conservation. *Nat. Rev. Microbiol.* 6, 579-591.
- Trotsenko, Y.A., Murrell, J.C., 2008. Metabolic aspects of aerobic obligate methanotrophy. In: Laskin, A.I., Sariaslani, S., Gadd, G.M. (Eds.), *Advances in Applied Microbiology*. Academic Press, pp.183-217.
- Unnikrishnan, A.S., Antony, M.K., 1990. On the vertical velocity fluctuations and internal tides in an upwelling region of the West coast of India. *Estuar. Coast. Shelf Sci.* 31, 865–873.
- Yadav, D.N., 1996. Manganese mobilization from the Western continental margin of India. *Curr. Sci.* 71, 900-905.
- Wang, Q., Alowaifeer, A., Kerner, P., Balasubramanian, N., Patterson, A., Christian, W., Tarver, A., Dore, J.E., Hatzenpichler, R., Bothner, B., McDermott, T.R., 2021. Aerobic bacteria methane synthesis. *PNAS* 118 (27), e2019229118.
- Weber, T., Wiseman, N.A., Kock, A., 2019. Global ocean methane emissions dominated by shallow coastal waters. *Nat. Comm.* 10, 4584.
- Wegener, G., Krukenberg, V., Riedel, D., Tegetmeyer, H.E., Boetius, A., 2015. Intercellular wiring enables electron transfer between methanotrophic archaea and bacteria. *Nature* 526, 587–590.
- Zehnder, A.J.B., Brock, T.D., 1979. Methane formation and methane oxidation by methanogenic bacteria. *J. Bacteriol.* 137, 420-432.

Żygadłowska, O.M., Venetz, J., Klomp, R., Lenstra, W.K., van Helmond, N.A.G.M., Röckmann, T., Wallenius, A.J., Martins, P.D., Veraart, A.J., Jetten, M.S.M., Slomp, C.P., 2023. Pathways of methane removal in the sediment and water column of a seasonally anoxic eutrophic marine basin. *Front. Mar. Sci.* 10:1085728, doi: 10.3389/fmars.2023.1085728

Żygadłowska, O.M., Roth, F., van Helmond, N.A.G.M., Lenstra, W.K., Venetz, J., Dotsios, N., Röckmann, T., Veraart, A.J., Stranne, C., Humborg, C., Jetten, M.S.M., Slomp, C.P., 2024. Eutrophication and deoxygenation drive high methane emissions from a brakish coastal system. *Environ. Sci. Technol.* 58, 10582-10590.

Tables

Table 1. Location of the stations. Tick mark denotes the depths at which the whole core incubation and CH₄-spiked ¹⁵N incubations were carried out.

| Transect Location | Station | Latitude (N) | Longitude (E) | Depth (m) | Whole core incubation | CH ₄ -spiked ¹⁵ N incubation |
|-------------------|---------|--------------|---------------|-----------|-----------------------|--|
| Off Mumbai | B2 | 18° 4.567' | 72° 43.844' | 34 | | ✓ |
| Off Goa | G3 | 15° 31.044' | 73° 43.930' | 6 | | ✓ |
| | | | | 13 | | ✓ |
| Off Goa | G4 | 15° 30.968' | 73° 42.804' | 7 | | ✓ |
| | | | | 15 | | ✓ |
| Off Goa | G5 | 15° 30.530' | 73° 38.97' | 14 | | ✓ |
| | | | | 20 | | ✓ |
| | | | | 25 | ✓ | ✓ |
| Off Goa | G6 | 15° 29.98' | 73° 34.880' | 28 | | ✓ |
| | | | | 34 | | ✓ |
| Off Karwar | K3 | 14° 28.1' | 74° 10.13' | 20 | | ✓ |
| | | | | 30 | | ✓ |
| Off Mangalore | M1 | 13° 8.47' | 74° 38.354' | 15 | | ✓ |
| | | | | 22 | ✓ | |
| | M3 | 13° 8.417' | 74° 33.46' | 25 | | ✓ |
| Off Calicut | C1 | 11° 20.22' | 75° 36.23' | 7 | | ✓ |
| | | | | 15 | | ✓ |

Table 2. Mean rates of pelagic CH₄ production/consumption with standard deviation (in parenthesis) measured through shipboard incubations at G5 (off Goa) and M1 (off Mangalore). Positive rates denote production, and negative rates denote consumption.

| Incubation | G5, February 2013 | | M1, February 2013 | | G5, October 2013 | | M1, October 2024 | |
|-------------------|---|---|---|---|---|---|---|---|
| | CH ₄ production/ consumption rate | | CH ₄ production/ consumption rate | | CH ₄ production/ consumption rate | | CH ₄ production/ consumption rate | |
| | (nmol L ⁻¹ h ⁻¹) | (μ mol m ⁻² d ⁻¹) | (nmol L ⁻¹ h ⁻¹) | (μ mol m ⁻² d ⁻¹) | (nmol L ⁻¹ h ⁻¹) | (μ mol m ⁻² d ⁻¹) | (nmol L ⁻¹ h ⁻¹) | (μ mol m ⁻² d ⁻¹) |
| Water (aerobic) | -0.137 (\pm 0.01) | -0.84 (\pm 0.07) | 0.082 (\pm 0.004) | 0.51 (\pm 0.01) | <i>not measured</i> | <i>not measured</i> | <i>not measured</i> | <i>not measured</i> |
| Water (anaerobic) | 0.095 (\pm 0.007) | 0.57 (\pm 0.01) | 0.211 (\pm 0.01) | 1.27 (\pm 0.03) | 0.106 (\pm 0.003), -0.028 (\pm 0.002) | 0.62 (\pm 0.04), -0.16 (\pm 0.01) | 0.102 (\pm 0.01) | 0.6 (\pm 0.007) |

Table 3. Mean rates of benthic CH₄ flux with standard deviation (in parenthesis) measured through shipboard whole-core incubations at G5 (Off Goa) and M1 (off Mangalore). Positive rates denote efflux (sediment to water), and negative rates denote influx (water to sediment).

| Incubation | G5, February 2013 | Benthic CH ₄ flux rate (μmol m ⁻² d ⁻¹) | | |
|----------------------------|-------------------|---|---------------------|---------------------|
| | | M1, February 2013 | G5, October 2013 | M1, October 2024 |
| Sediment-water (aerobic) | -0.23 (±0.06) | 0.37 (±0.02) | <i>not measured</i> | <i>not measured</i> |
| Sediment-water (anaerobic) | 2.55 (±0.06) | 74.05 (±0.3) | 2.35 (±0.21) | 76.34 (±2.2) |
| Sediment-water (poisoned) | 25.49 (±1.8) | 152.18 (±5.7) | 22.16 (±1.1) | 156.33 (±1.9) |

Table 4. A comparative analysis of maximum CH₄ concentration in the bottom water and benthic CH₄ flux rates among various shallow anoxic coastal systems of the world. N.M.: not measured.

| Anoxic coastal system, Location | Maximum bottom water CH ₄ (nM) | Benthic CH ₄ flux rate (μmol m ⁻² d ⁻¹) | Reference |
|-----------------------------------|---|---|---|
| Mariager Fjord, Denmark | 1400 ^a | 300-1500 ^b | Steinsdóttir et al. (2022a) ^a , Fenchel et al. (1995) ^b |
| Randers Fjord, Denmark | 124 | 393-413 | Abril and Iversen (2002) |
| Namibian Shelf | 5300 | 40-18700 | Brüchert et al. (2009) |
| Baltic Sea | 3288 ^c | 2-3.7 ^d | Ketzer et al. (2024) ^c , Bonaglia et al. (2017) ^d |
| Saanich Inlet, Canada | 1300 | N.M. | Capelle et al. (2019) |
| Chilean Shelf | 101 | N.M. | Fariás et al. (2021) |
| By Fjord, Sweden | 5000 | 65-1029 | Bonaglia et al. (2022) |
| Golfo Dulce, Costa Rica | 1700 | N.M. | Steinsdóttir et al (2022b) |
| Lake Grevelingen, The Netherlands | 227000 | 1100-2700 | Żygadłowska et al. (2023) |
| Stockholm Archipelago, Sweden | 80000 | 2200-8600 | Żygadłowska et al. (2024) |
| Western Indian Shelf | 133 | 2.35-74.05 | This study |

Figures

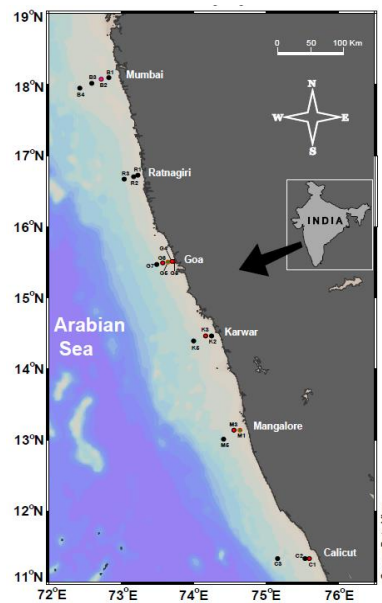


Fig.1. Location of the study area. Dots denote the stations where the water column biogeochemical parameters were measured. Red dots denote the stations where ^{15}N incubation was done and green dots the stations where benthic CH_4 flux was measured.

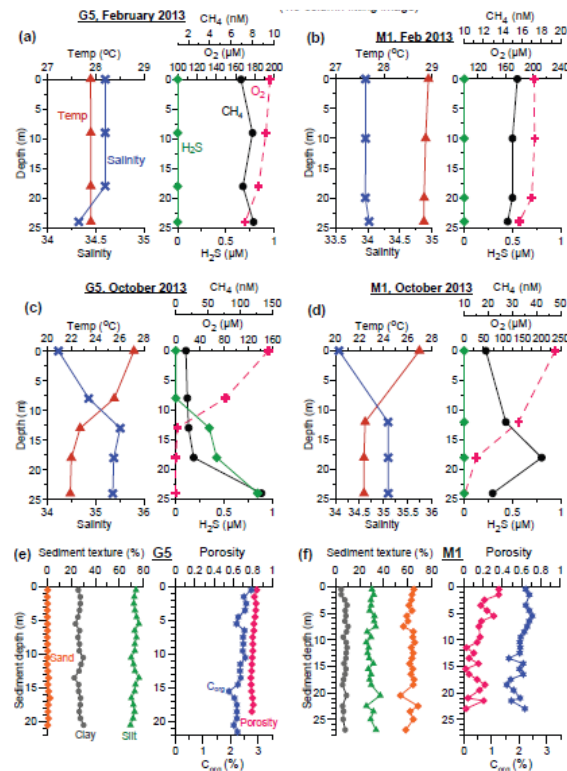


Fig. 2. Physico-chemical condition of the shelf water column during February 2013 (a, b) and October 2013 (c, d), and solid phase properties of the shelf sediments (e, f). Sediment texture, porosity and C_{org} data at G5 have been taken from Naik et al. (2017).

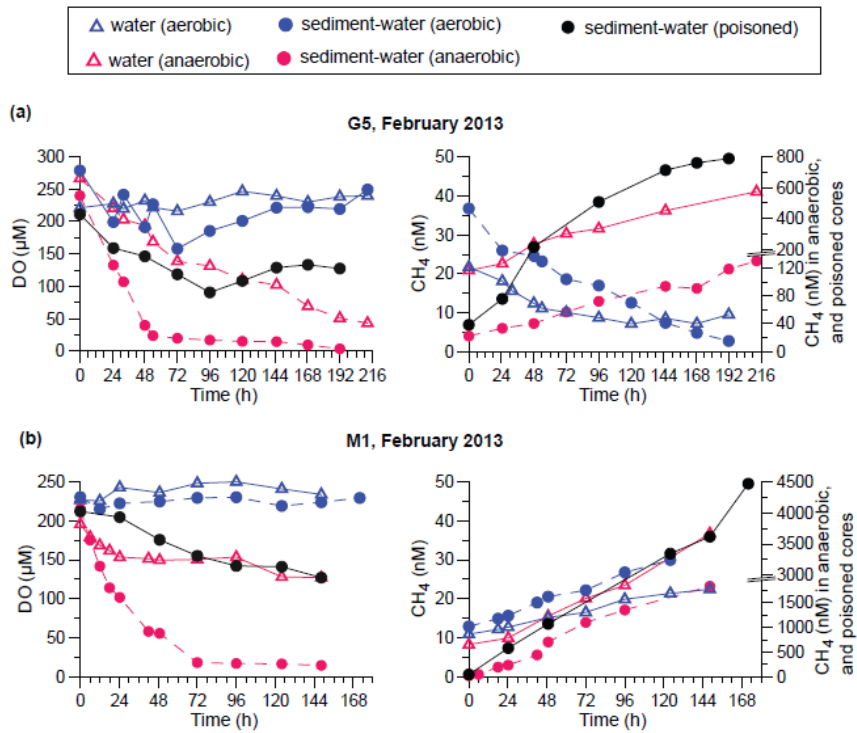


Fig.3. Variation in mean O_2 and CH_4 in the replicate water and sediment-water systems under aerobic, anaerobic, and poisoned conditions during February at (a) G5 (off Goa), and (b) at M1 (off Mangalore).

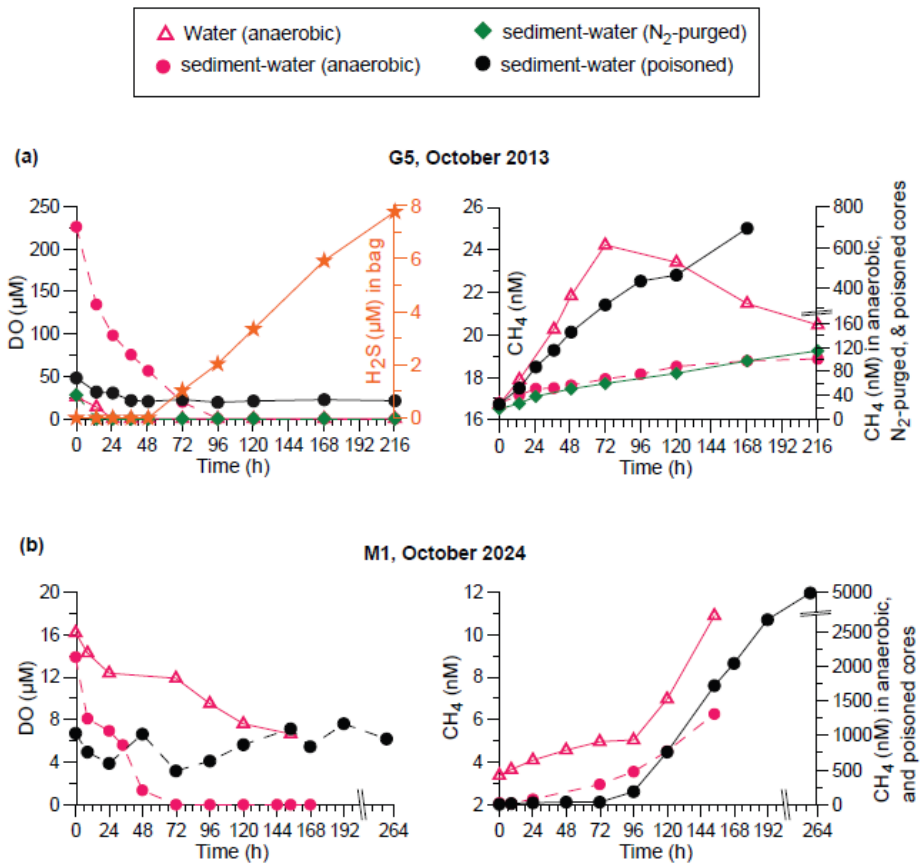


Fig.4. Variation in mean O_2 and CH_4 in the replicate water and sediment-water systems under anaerobic and poisoned condition during October at (a) G5 (off Goa), and (b) at M1 (off Mangalore).

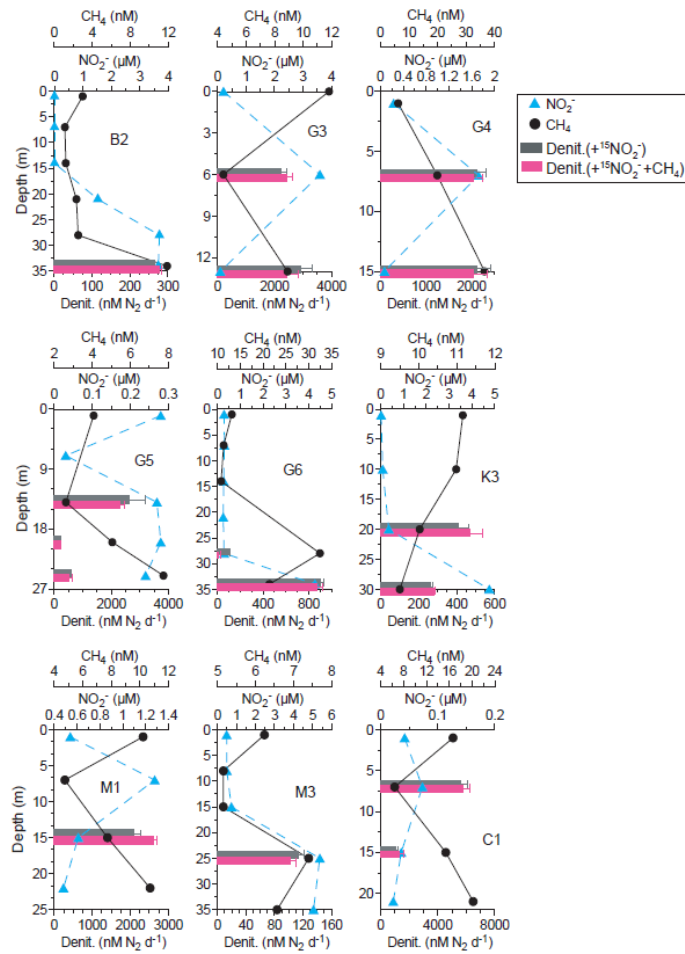


Fig.5. Vertical profiles of NO_2^- , CH_4 , and denitrification rates (Denit.) with and without CH_4 addition in the WICS waters during September-October 2011. NO_2^- data and denitrification rate without CH_4 addition have been taken from Pratihary et al. (2023).

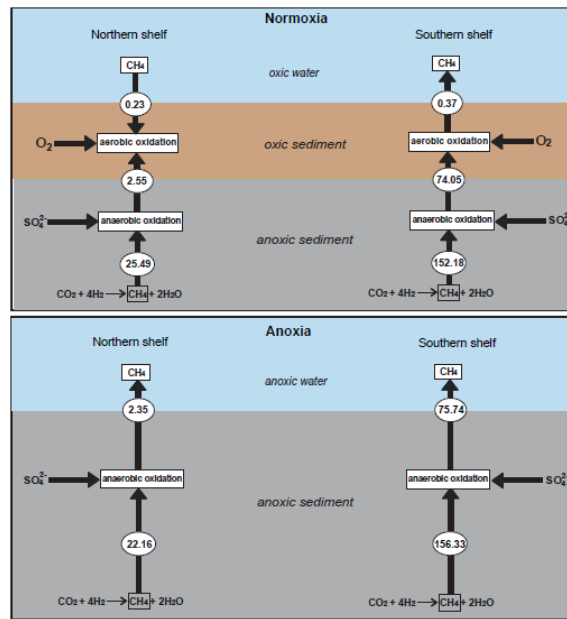


Fig.6. Schematic diagram showing the pathways and rates of methane oxidation in the WICS sediments during normoxia and anoxia.

Suppl. Table 1. Denitrification rates (SD in parenthesis) with and without CH₄ addition in the WICS waters as determined through ¹⁵N-incubations.

| Station | Depth (m) | Denitrification with ¹⁵ NO ₂ ⁻ (nmol N ₂ L ⁻¹ d ⁻¹) | Denitrification with ¹⁵ NO ₂ ⁻ +CH ₄ (nmol N ₂ L ⁻¹ d ⁻¹) |
|---------|-----------|---|--|
| B2 | 34 | 261 (±2.8) | 276 (±7.8) |
| G3 | 6 | 2242 (±184) | 2443 (±6.6) |
| | 13 | 2921 (±388) | 2429 (±60) |
| G4 | 7 | 2106 (±165) | 2048 (±196) |
| | 15 | 2120 (±37) | 2044 (±285) |
| G5 | 14 | 2646 (±551) | 2286 (±167) |
| | 20 | 221 (±6.8) | 189 (±19) |
| | 25 | 544 (±78) | 522 (±99) |
| G6 | 28 | 104 (±18) | 12 (±5.3) |
| | 34 | 901 (±50) | 875 (±27) |
| K3 | 20 | 408 (±63) | 471 (±53) |
| | 30 | 264 (±5.5) | 280 (±9.3) |
| M1 | 15 | 2079 (±192) | 2620 (±72) |
| M3 | 25 | 114 (±7.9) | 102 (±8.3) |
| C1 | 7 | 5573 (±531) | 5760 (±515) |
| | 15 | 1087 (±104) | 1309 (±301) |